

1 **Supplementary information**

2 **Depsipeptide Aspergillicins Revealed by Chromatin Reader Protein**
3 **Deletion**

4 C. Greco,^a B. T. Pfannenstiel,^b J. C. Liu^a and N. P. Keller^{a,c}

5 ^a Department of Medical Microbiology and Immunology, University of Wisconsin-Madison,
6 Madison, WI, USA

7 ^b Department of Genetics, University of Wisconsin-Madison, Madison, WI, USA

8 ^c Department of Bacteriology, University of Wisconsin-Madison, Madison, WI, USA

9

10 **Contents**

11	List of Tables	3
12	Experimental section.....	5
13	General procedures.....	5
14	HPLC-DAD	5
15	UHPLC-HRMS	5
16	Fungal strains and media	6
17	DNA fragment construction for gene disruption	6
18	Growth conditions and method of extraction	8
19	Bioinformatic analysis.....	8
20	Analysis of the thioesterase (TE) domains.....	12
21	Fungal transformation.....	12
22	Transformant confirmation.....	13
23	Semi quantitative PCR and quantitative PCR	14
24	Feeding experiment.....	15
25	Sensitivity to iron experiment.....	16
26	Isolations of aspergillicins	17
27	HRMS and UV spectra	19

28	NMR data	21
29	Reference	31
30		
31	List of Figures	
32	Figure S1. <i>A. flavus</i> Δ <i>sntB</i> (left) and wild type (right) strains grown on GMM for 6 days at 30 °C.	
33	6
34	Figure S2. Schematic of the aspergillicin BGC flanked by siderophores genes.....	8
35	Figure S3. ACT analysis of the aspergillicin BGC from <i>A. flavus</i> genome vs <i>A. oryzae</i>	9
36	Figure S4. ACT analysis of the aspergillicin BGC from <i>A. flavus</i> genome vs <i>A. arachidicola</i> . In <i>A.</i>	
37	<i>arachidicola</i> the BGC is split across two contigs.	9
38	Figure S5. ACT analysis of the aspergillicin BGC from <i>A. flavus</i> genome vs <i>A. nidulans</i>	9
39	Figure S6. ACT analysis of the aspergillicin BGC from <i>A. flavus</i> genome vs <i>A. fumigatus</i>	10
40	Figure S7. Multigene BLAST analysis of the aspergillicin BGC. The siderophore genes can be	
41	identified across different fungi.....	10
42	Figure S8. Multiple sequence alignment done using Clustal Omega. Red box highlights conserved	
43	motif.....	11
44	Figure S9. Phylogenetic tree for the TE domains (orange) and C domains (blue). Dark orange	
45	highlights fungal NRPS-TE domains. The TE domains is divided in bacterial TEs, fungal NRPS-	
46	TE and fungal PKS-TE domains.	12
47	Figure S10. Schematic of the expected product from digestion using <i>MfeI</i> and <i>HindIII</i> (left).	
48	Southern results for Δ <i>agiA</i>	13
49	Figure S11. PCR confirmation of the correct disruption of the resistance and purity. Schematic of	
50	the expected product (left). Gel for the transformants C = control; W = water, T = transformants.	
51	Purity test indicates primer that amplify the ORF, and no product should be observed in the correct	
52	transformants. Δ <i>agiB</i> ; T1 correct LH (2500 bp), RH (1744 bp), and no product in purity test (1286	
53	bp). Δ <i>sidJ</i> ; T2 correct LH (2426 bp), RH (2005 bp), and no product in purity test (2490 bp). Δ <i>agiB</i> ;	
54	T1, T2, T3, T4, T5 correct LH (2861 bp), RH (1730 bp), and no product in purity test (3034 bp).	
55	14
56	Figure S12. A) Semi-qPCR analysis for <i>agiA</i> , <i>agiB</i> , <i>sidJ</i> , <i>sidF</i> and <i>acting</i> (expected products 100-	
57	120 bp). B) Bar charts showing relative expression of <i>agiA</i> , <i>agiB</i> and <i>sidJ</i> using normalized	
58	expression ration ($2^{-\Delta\Delta C_t}$ Method) between WT and Δ <i>sntB</i>	15

59	Figure S13. Summary of the feeding experiment using O-Me-L-tyrosine. $\Delta sntB$ produces	
60	aspergillicin A 1 and F 2. $\Delta sntB\Delta agiB$ produces aspergillicin C 4 and aspergillicin G 11.	
61	$\Delta sntB\Delta agiB$ plus O-Me-tyrosine produces aspergillicin A 1 and aspergillicin F 2.....	16
62	Figure S14. GMM plates containing different amounts of $FeSO_4$ (0, 5 μM , 1 mM and 10 mM)	
63	inoculated with WT and Δsnt , $\Delta sntB\Delta agiA$, $\Delta sntB\Delta agiB$, $\Delta sntB\Delta sidF$ and $\Delta sntB\Delta agiJ$. Picture taken	
64	after 5 days.....	16
65	Figure S15. HRMS spectrum (left) and UV spectrum of aspergillicin A 1.....	19
66	Figure S16. HRMS spectrum (left) and UV spectrum of aspergillicin F 2.....	19
67	Figure S17. HRMS spectrum (left) and UV spectrum of aspergillicin B 4.....	20
68	Figure S18. HRMS spectrum (left) and UV spectrum of aspergillicin G 11.	20
69	Figure S19. 1H NMR of aspergillicin A 1 (600 MHz in $CDCl_3$).....	23
70	Figure S20. ^{13}C NMR of aspergillicin F 1 (150 MHz in $CDCl_3$).....	23
71	Figure S21. HSQC spectrum of aspergillicin A 1 (600 MHz in $CDCl_3$).....	24
72	Figure S22. HMBC spectrum of aspergillicin A 1 (600 MHz in $CDCl_3$).....	24
73	Figure S23. 1H NMR of aspergillicin F 1 (600 MHz in $CDCl_3$).....	25
74	Figure S24. ^{13}C NMR of aspergillicin F 2 (150 MHz in $CDCl_3$).....	25
75	Figure S25. COSY spectrum of aspergillicin F 2 (600 MHz in $CDCl_3$).....	26
76	Figure S26. HSQC spectrum of aspergillicin F 2 (600 MHz in $CDCl_3$).....	26
77	Figure S27. HMBC spectrum of aspergillicin F 2 (600 MHz in $CDCl_3$).....	27
78	Figure S28. 1H NMR of aspergillicin C 4 (600 MHz in $CDCl_3$).....	27
79	Figure S29. COSY spectrum of aspergillicin C 4 (600 MHz in $CDCl_3$).....	28
80	Figure S30. ^{13}C NMR of aspergillicin G 11 (150 MHz in $CDCl_3$).....	28
81	Figure S31. 1H NMR of aspergillicin G 11 (600 MHz in $CDCl_3$).....	29
82	Figure S32. COSY spectrum of aspergillicin G 11 (600 MHz in $CDCl_3$).....	29
83	Figure S33. HSQC spectrum of aspergillicin G 11 (600 MHz in $CDCl_3$).....	30
84	Figure S34. HMBC spectrum of aspergillicin G 11 (600 MHz in $CDCl_3$).....	30

85 List of Tables

86	Table S1. List of strain used in this work.....	6
87	Table S2. List of oligonucleotides.....	7
88	Table S3. Summary of the predicted functions for the genes in the putative aspergillicin cluster.	
89	The function was determined using NCBI BLAST in non-redundant database.....	8
90	Table S4. NMR assignment of aspergillicin F 2 in agreement with literature ⁸ (^a 150 MHz, ^b 600 MHz	
91	in $CDCl_3$).....	21

92	Table S5. NMR assignment of aspergillicin G 11 (^a 150 MHz, ^b 600 MHz in CDCl ₃)......	22
93		

94 **Experimental section**

95 **General procedures**

96 Analytical grade chemicals and reagents were supplied from Sigma-Aldrich, Alfa Aesar, Acros
97 Organics and Fischer, unless otherwise stated. Solvents used for HPLC-DAD analyses were
98 HPLC grade, and for UPLC-HRMS analysis were LCMS grade. General molecular biology
99 procedures were performed as standard and molecular biology kits used according to
100 manufacturer's protocols. Analytical PCR was performed using Pfull Ultra high fidelity (Agilent)
101 Expand Long Template PCR (Roche) DNA polymerases.

102 **NMR**

103 NMR experiments were conducted on the following spectrometers: Bruker Avance-500 DCH
104 cryoprobe (^1H NMR at 500 MHz and ^{13}C NMR at 125 MHz), Bruker Avance-600 TCI-F cryoprobe
105 (^1H NMR at 500 MHz and ^{13}C NMR at 150 MHz). Chemical shifts were recorded in parts per
106 million (ppm referenced to the appropriate residual solvent peak).

107 **HPLC-DAD**

108 HPLC-DAD for analysis and purification was performed on Gilson GX-271 Liquid Handler with
109 system 322 H2 Pump connected to a 171 Gilson Diode Array Detector and fraction collector. A
110 XBridge BEH C18 XP Column (130 Å, 2.5 μm , 4.6 mm x 100 mm) with XBridge BEH C18 XP
111 VanGuard Cartridge (130 Å, 2.5 μm , 3.9 mm x 5 mm) was used for analytical run with a flow rate
112 of 0.8 mL/min. A XBridge BEH C18 OBD Prep Column (130 Å, 5 μm , 19 mm x 250 mm) with a
113 XBridge BEH C18 Prep Guard Cartridge (130 Å, 5 μm , 19 mm x 10 mm) was used for preparative
114 run with flow rate of 16 mL/min. HPLC grade water with 0.5% formic acid (solvent A) and HPLC
115 grade acetonitrile with 0.5% formic acid (solvent B) were used with the following gradient 0 min,
116 20% Solvent B; 2 min, 20% Solvent B; 15 min, 95% Solvent B; 20 min, 95% Solvent B; 20 min,
117 20% Solvent B; 25 min, Solvent B. Data acquisition and procession for the HPLC-DAD were
118 controlled by TRILUTION LC V3.0.

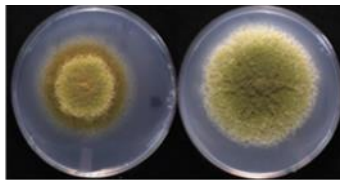
119 **UHPLC-HRMS**

120 UHPLC-HRMS was performed on a Thermo Scientific-Vanquish UHPLC system connected to a
121 Thermo Scientific Q Exactive Orbitrap mass spectrometer in ES^+ and ES^- mode between 200 m/z
122 and 1000 m/z to identify metabolites. A Zorbax Eclipse XDB-C18 column (2.1 \times 150 mm, 1.8 μm
123 particle size) was used with a flow rate of 0.2 mL/min for all samples. LCMS grade water with
124 0.5% formic acid (solvent A) and LCMS grade acetonitrile with 0.5% formic acid (solvent B) were

125 used with the following gradient 0 min, 20% Solvent B; 2 min, 20% Solvent B; 15 min, 95% Solvent
 126 B; 20 min, 95% Solvent B; 20 min, 20% Solvent B; 25 min, Solvent B. Nitrogen was used as the
 127 sheath gas. Data acquisition and procession for the UHPLC-MS were controlled by Thermo
 128 Scientific Xcalibur software.

129 Fungal strains and media

130 Strains used in this study are listed in Supplementary Table S1. They were grown on glucose
 131 minimal media (GMM)¹ with additional supplements for auxotrophic strains. Solid and liquid
 132 cultures were grown in a light incubator at 30 °C. All strains were maintained as glycerol stocks
 133 at -80 °C. Strain TJW149 is used as our wild-type control unless otherwise noted.



134
 135 **Figure S1.** *A. flavus* $\Delta sntB$ (left) and wild type (right) strains grown on GMM for 6 days at 30 °C.

136 **Table S1.** List of strain used in this work.

Strain Name	Genotype	Reference
TJW149	$\Delta ku70::A. parasiticus pyrG$	2
TJES20.1	$\Delta ku70; pyrG^-; \Delta argB::A. fumigatus pyrG$	3
TXZ13	$\Delta ku70; pyrG^-; \Delta argB; \Delta sntB::A. flavus argB$	3
TXZ14	$\Delta ku70:: A. fumigatus pyrG; pyrG^-; \Delta argB; \Delta sntB::A. flavus argB$	3
TCG3.1	$\Delta ku70; pyrG^-; \Delta argB; \Delta sntB::A. flavus argB; \Delta agiA::A. fumigatus pyrG$	This study
TCG4.1	$\Delta ku70; pyrG^-; \Delta argB; \Delta sntB::A. flavus argB; \Delta agiB::A. fumigatus pyrG$	This study
TCG5.1	$\Delta ku70; pyrG^-; \Delta argB; \Delta sntB::A. flavus argB; \Delta sidJ::A. fumigatus pyrG$	This Study
TCG6.1	$\Delta ku70; pyrG^-; \Delta argB; \Delta sntB::A. flavus argB; \Delta sidF::A. fumigatus pyrG$	This study

137

138 DNA fragment construction for gene disruption

139 All the DNA constructs were prepared using double joint PCR.⁴ 1 to 2 kb of 5' and 3' flanking
 140 sequence of each gene of interest was amplified using oligonucleotides listed in Table S2 (i.e.,
 141 5'-F paired with 5'-R) from RAAS233.2 genomic DNA, with the *pyrG* marker amplified from
 142 genomic DNA isolated from *A. fumigatus*. These fragments were then fused together *via* PCR to

143 generate deletion constructs. PCR amplification was carried out on a C1000TM Thermal Cycler
 144 (BioNRad).

145 **Table S2.** List of oligonucleotides

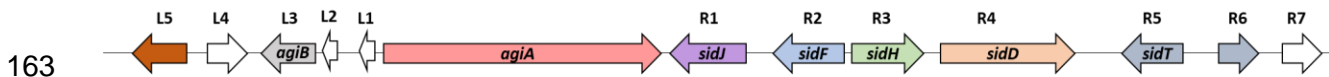
Name	Sequence	Use
CG-pyrG-F	TGCTCTTCACCCCTCTTCGC	Selectable marker
CG-pyrG-R	CTGTCTGAGAGGAGGCACTG	Selectable marker
CG-agiA-5'-F	GAGTAGCAGGGCTTCTGTTC	Gene deletion
CG-agiA-5'-R	ATTTCCAGACCCGCGAAGAGGGTGAAGAGCACTCATCTGCTTC CAATCG	Gene deletion
CG-agiA-3'-F	GACAGTATAATACAAACAAAGATGCAAGAGGGATGTGTGCCATG TACGAG	Gene deletion
CG-agiA-3'-R	GTGCAGGTGGTGGTACATAA	Gene deletion
CG-agiA-5'-F-int	GCAGCGTTGACTTATTCGC	Gene deletion
CG-agiA-3'-R-int	GCCGCCATTTGTGTTGATAG	Gene deletion
CG-agiB-5'-F	GTGCAGTGAACGGTAGACTAG	Gene deletion
CG-agiB-5'-R	ATTTCCAGACCCGCGAAGAGGGTGAAGAGCAGGAGCCCGAATCA AGTCTC	Gene deletion
CG-agiB-3'-F	CATCACGCATCAGTGCCTCCTCTCAGACAGATGGTTGGGAGTC AGGATGC	Gene deletion
CG-agiB-3'-R	GCCAGAAAGCCCTCGGAATAG	Gene deletion
CG-agiB-5'-F-int	GCTTCGGGAGTTCGGATC	Gene deletion
CG-agiB-3'-R-int	GGTGTATCCTTGCCAGTTCAC	Gene deletion
CG-sidJ-5'-F	CACAGCGCGAAAGTACGATG	Gene deletion
CG-sidJ-5'-R	ATTTCCAGACCCGCGAAGAGGGTGAAGAGCAGGCCGTGAAGGATA TCGCTATG	Gene deletion
CG-sidJ-3'-F	CATCACGCATCAGTGCCTCCTCTCAGACAGCCAGGAGAATCCG GACTATCG	Gene deletion
CG-sidJ-3'-R	CTAGGGCCATAGTATTCTCCG	Gene deletion
CG-sidJ-5'-F-int	CTGTAAAAGCCTCTGTGGCG	Gene deletion
CG-sidJ-3'-R-int	CACCTCGTGTCTGGAATCTG	Gene deletion
CG-sidF-5'-F	GGCATTCAACATAGGGACCG	Gene deletion
CG-sidF-5'-R	ATTTCCAGACCCGCGAAGAGGGTGAAGAGCAGCTGTAAAGTCAG AGGGATGC	Gene deletion
CG-sidF-3'-F	CATCACGCATCAGTGCCTCCTCTCAGACAGGCCCTGGTTTATAT CTGAGCAA	Gene deletion
CG-sidF-3'-R	CAGACCACTCAGTGCATCTC	Gene deletion
CG-sidF-5'-F-int	TGTTGTAGCCTTATCCAAGCG	Gene deletion
CG-sidF-3'-R-int	GCGACGACAATATCGCAATTG	Gene deletion
CG-agiB-Check-F	CGTGCCTTCATTGCACTGA	Check mutant
CG-agiB-Check-R	CCAAATCGGTAACCTAAGGCGA	Check mutant
CG-agiB-pur-R	CGTCCTTACAGGTACGACAG	Check mutant
CG-sidJ-Check-F	GTAGCCTGAGATCGGCTTC	Check mutant
CG-sidJ-Check-R	CGTACCAGTATCCAGACGGT	Check mutant
CG-sidJ-pur-R	CCGATTGGGTTGATAAGGAGC	Check mutant
CG-sidJ-Check-F	GATGCCGTTGGGTATGCAAT	Check mutant
CG-sidJ-Check-R	GGAGACCCCTCCATCGTAAC	Check mutant
CG-NacT-pur-R	CCACGAGTGCTTCAGCT	Check mutant
PyrG-Check-F	GCATCGGTTGACTACGCT	Check mutant
PyrG-Check-R	CGAGCGTAGTCAACCGAT	Check mutant
CG-actin-semi-F	CCACGTTACCACCTTCAACTC	qPCR
CG-actin-semi-R	GGAGATGCCAGGGTACATGG	qPCR
CG-agiA-semi-F	GCGTGTGTTGACCATGTGGTGC	qPCR
CG-agiA-semi-R	GCGCTTCCAAGTAATGTGCGG	qPCR
CG-agiB-semi-F	GCCGCCGTACAAACACATCATATC	qPCR
CG-agiB-semi-R	GGCAATGAACCCTCACCAGAG	qPCR
CG-sidJ-semi-F	CAATCGGGAACCGCTGATCC	qPCR
CG-sidJ-semi-R	CGGATTTGAGTGAGGAGCAGC	qPCR
CG-sidF-semi-F	GGACAGAGCGCTTATGCCAG	qPCR
CG-sidF-semi-R	GCCGAAGGCGACGAATACAA	qPCR

147 **Growth conditions and method of extraction**

148 The *A. flavus* strains were grown on glucose minimal media (GMM), potato dextrose agar (PDA)
 149 or potato dextrose broth (PDB) for 14 days at 30 °C, the liquid culture was shaken at 200 rpm.
 150 Each 25 mL plate was blended in ethyl acetate (100 mL) and water (50 mL). After two hours, the
 151 solid was removed using vacuum filtration and the organic layer was separated. The aqueous
 152 layer was extracted with ethyl acetate (2 x 25 mL). The combined organic phases were dried over
 153 anhydrous magnesium sulfate and concentrated under reduced pressure. To a liquid PDB culture
 154 (200 mL), ethyl acetate (300 mL) was added. The mixture was blended and left soaking for 2
 155 hours. The mycelia were removed by vacuum filtration, the organic layer was removed, and the
 156 aqueous layer was extracted with ethyl acetated (2 x 100 mL). The combined organic phases
 157 were dried over anhydrous magnesium sulfate and concentrated under reduced pressure. The
 158 dried extracts were resuspended in LCMS grade acetonitrile at a concentration of 10 mg/mL and
 159 filtered through an Acrodisc syringe filter with a nylon membrane (Pall Corporation) (0.45 µm pore
 160 size).

161 **Bioinformatic analysis**

162 **Analysis cluster**



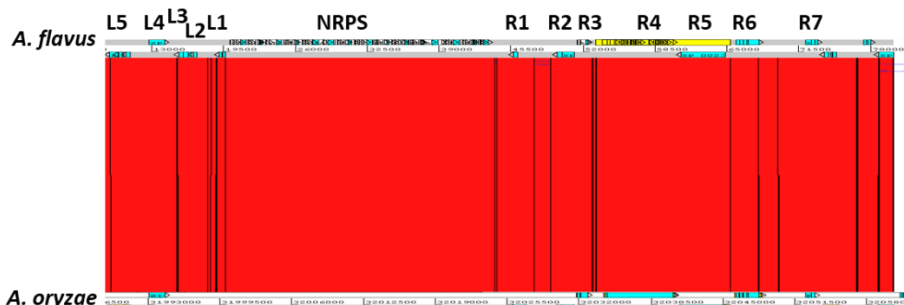
164 **Figure S2.** Schematic of the aspergillicin BGC flanked by siderophores genes.

165 **Table S3.** Summary of the predicted functions for the genes in the putative aspergillicin cluster. The function was
 166 determined using NCBI BLAST in non-redundant database.

Gene	Putative function	Homolog	Gene identity	Query coverage
L5	Hypothetical protein	<i>A. bombycis</i>	65%	85%
L4	Lipase 2	<i>A. nomius</i> NRRL 13137 <i>A. arachidicola</i>	88% 84%	99% 99%
L3	O-methyl transferase	<i>A. bombycis</i> <i>A. arachidicola</i>	92% 86%	99% 99%
L2	Hypothetical protein	<i>A. bombycis</i>	88%	96%
L1	Hypothetical protein	<i>A. arachidicola</i>	92%	98%
NRPS	NRPS (AFLA_010580)	<i>A. arachidicola</i> <i>A. bombycis</i>	95% 81%	99% 99%
R1	esterase	<i>A. arachidicola</i>	99%	99%
R2	Acetylase AceI N-acyltransferase	<i>A. arachidicola</i>	98%	96%
R3	enoyl-CoA hydratase	<i>A. arachidicola</i>	98%	99%
R4	nonribosomal siderophore peptide synthase Sid2	<i>A. arachidicola</i>	96%	99%
R5	ABC transporter sidT	<i>A. arachidicola</i>	99%	99%
R6	MFS transporter mirB	<i>A. arachidicola</i>	99%	99%
R7	Hypothetical protein	<i>A. bombycis</i>	78%	98%
R8	Hypothetical protein	<i>A. bombycis</i>	78%	99%

167 **Artemis comparison tool (ACT) analysis**

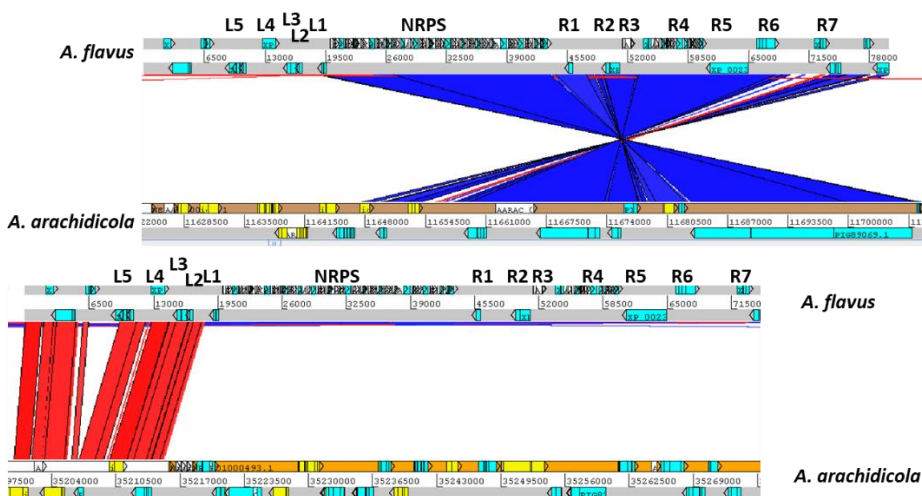
168 ACT⁵ was used to compare the aspergillacin BGC from *A. flavus*. to the genome of *A. fumigatus*,
169 *A. oryzae*, *A. arachidicola* and *A. nidulans*. The red and blue lines indicate homologous genes
170 with identity above 75%.



171

172

Figure S3. ACT analysis of the aspergillacin BGC from *A. flavus* genome vs *A. oryzae*.

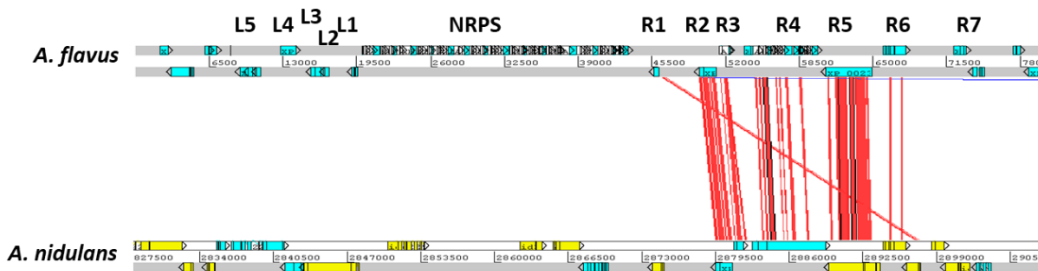


173

174

175

Figure S4. ACT analysis of the aspergillacin BGC from *A. flavus* genome vs *A. arachidicola*. In *A. arachidicola* the BGC is split across two contigs.

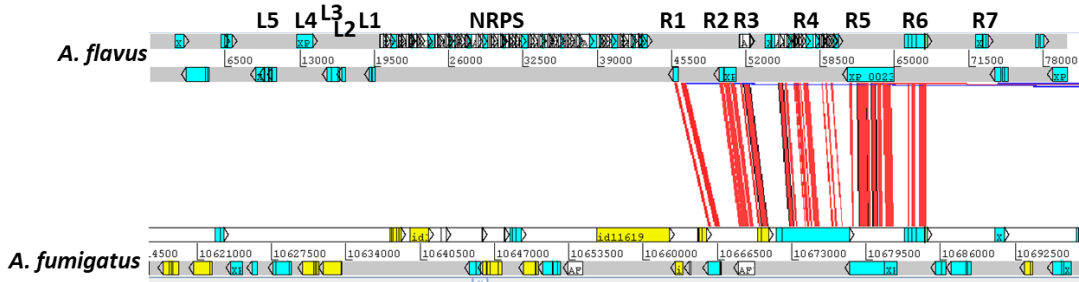


176

177

Figure S5. ACT analysis of the aspergillacin BGC from *A. flavus* genome vs *A. nidulans*.

178



179

180

Figure S6. ACT analysis of the aspergillacin BGC from *A. flavus* genome vs *A. fumigatus*.

181 Multigene BLAST

182 Multigene BLAST⁶ analysis identified that the siderophore BGC is fairly conserved across many
183 fungi. But the NRPS *agiA* is unique to *A. flavus* and closely related species.



184

185 Figure S7. Multigene BLAST analysis of the aspergillacin BGC. The siderophore genes can be identified across different
186 fungi.

187

188 Analysis of condensation domain

189 Multiple sequence alignment using Clustal Omega of the condensation domains of AgiA
190 (AFLA_010580) revealed the canonical HHxxxDG motif.

CLUSTAL O(1.2.4) multiple sequence alignment

```

C5  --VRQSF AQGR LWF LDQLHPGSTWYLM PFGLRIQGD-LH L D A L E A A V S A I E E R H E T L R T T   57
C1  ---APSVMQEEMIVSTIADPSHKSYFETYHFS AQGI-VDPDQLNGAIHAVARKHAVLR SV   56
C3  DIIPCTPMQRALLYEGIADHESRSYVTCRIWRIPTDQAIC SQIEGAVKSLIQRHGILRTV   60
C2  AIYPCTPQQEGLIQTSLH-GDKSAYFATITVHLGDS-LNLRTFHAAWNR L VFGDMLRTA   58
C4  -VMPCTPFQEGVLSNDESGSSAGYLAHMTVGLGKE-IDVEALKYAWQETVDHEDMLRTT   58
C6  -LMPCTPFQEGVLSNSLAVPGDSGYLSVVR LGLQSQ-LDTKAMRLAWQKVVEREETLR TA   58
      : * : * . : * ** : .

C5  FEHRDGENVQVVHPFAH-RQLRVVEVPPAVDEEGLLGALKE-----   97
C1  FVHPTEFDSTNV-----QIAVLDQA-YTLHRAKLLSLQ-----PIGE   92
C3  FHIDPEVGPLA-----LVL RDTQSP TA-SAVGHVKVKDHTEMEERV-T-----SLLC   105
C2  FVSFSVQHPH---VSESNILQVVLSQSA-EDVRR LVS LDNRD-----I   98
C4  FIPADMMDTDIRLGGSSLLQVVLYPES-PQAGR VTKMTVSTPATPNAALPSYPSLQG   117
C6  FIPVAEDLSSACIT--SSTFWQCFININS-REVQRLLCIEGRN-----SG-----VDRS   104
      * : : .

C5  ---EQSTPFDLQVHPGWR-----PL--VLRQNKRS HILSIVHHIICDGN SVAVLLK   144
C1  EIRFGILPLESIGTDEWDGVM PWFSLVVC---EREQKSYITVRYHHALLDGN SARALLE   149
C3  NPDYGNPMKQAFYV-----RI--VHAADGSGARLIWLIHSLIDANSQDLLLS   151
C2  AFQFGVPLSAGI-----SQGSVNEPWRLHLKHHALYDEAFLSRIVA   141
C4  KAQQGHIPVAALVAI-----GSQDGEQECTLLITHHALYDEAYLSLLLK   163
C6  ALGFGHIPVSLILTDV-----PTVCKARGV-GSTQLELTHHALYDEAYFRWIIH   153
      : ** : * : :

C5  ELSTFYSAALHGKPIHA-QLPPLPIQYRDFS AWESQKEQR----VEHDRQLKYWIEKLTG   199
C1  LVQQEMLNPG-----AVLKGSDFFSLVRQPLK----RDWKQDETL LRERLAQ   192
C3  ELTQILVDG-----CP---TKSLIPRPSFGSFARYVTS D---SRADHSHGKFWSETLNG   199
C2  ELCIVYEAL EME SSEAA-----LPPSRPFSAFVESLCN----DDPEVSKGFWKYMH E   190
C4  DLSGRYRSIACNE-VVP---QVPEDQRIPFSTYVRFVH SKLGTAPSTSTAGKFWKSYLAD   219
C6  ELSREYHKARLAKDYVPLRAPQTS MNRI PF SIFVSQLQA-----MPKESATSFWKSYLNG   208
      : * : :

C5  SK--PAE--FIC--DKRRPQAPSRQAI FEE--VRIDGAMYDQLRQYCKQHQLTPFIVLLA   251
C1  IETSPILSPGPVANGD--LRVGEVTREVSISSDIW-----LPDRPAV PARLLRL   239
C3  VQ--PKS--LPLSLMSSSP-INAA-----AVVVEQACN-----LAILSENCISPAALVSL   244
C2  VA--PAT--WPV ASGIRRMREENGQDVEMTVVKS WTGNA---VALGQKFQATPASIVRA   242
C4  AT--PST--WPLPHGMQSS-ITSVKS-PETA VLEWTGNL----RAAASKVQV TAAAIARA   269
C6  AP--AAC--WPVARGLESGRITEIDE-FSSRS LIWKGNM----HNLAGARGVTPAAISRA   259
      :

C5  VFRATHYRLTREADATIGTPIANRGRE-----ELHDIIGLFVNVQCIRLKVD   298
C1  ALGMTISVFRNSDDSLFLEITSARSRL----FPKDQQVLGP-----   276
C3  AWSLVLSEILD TD D VTHGMLFSGRQLP---VD-GVADIIGPCISTVP I RTHL-   292
C2  ALALALAQYSQTDVVFGEVSSGRFDH-----DRFTLGPCLATHPVRIQI-   287
C4  ALALTVAEHTNVDVVLGEVSKGRPDIRGPGDARARFITGPCATTHPVRIR--   320
C6  AVALVVAEHS GVEDIVLGEVSSGRSIT----DGAAGFVAGPCISTHP I RIM-   307
      * * * * *

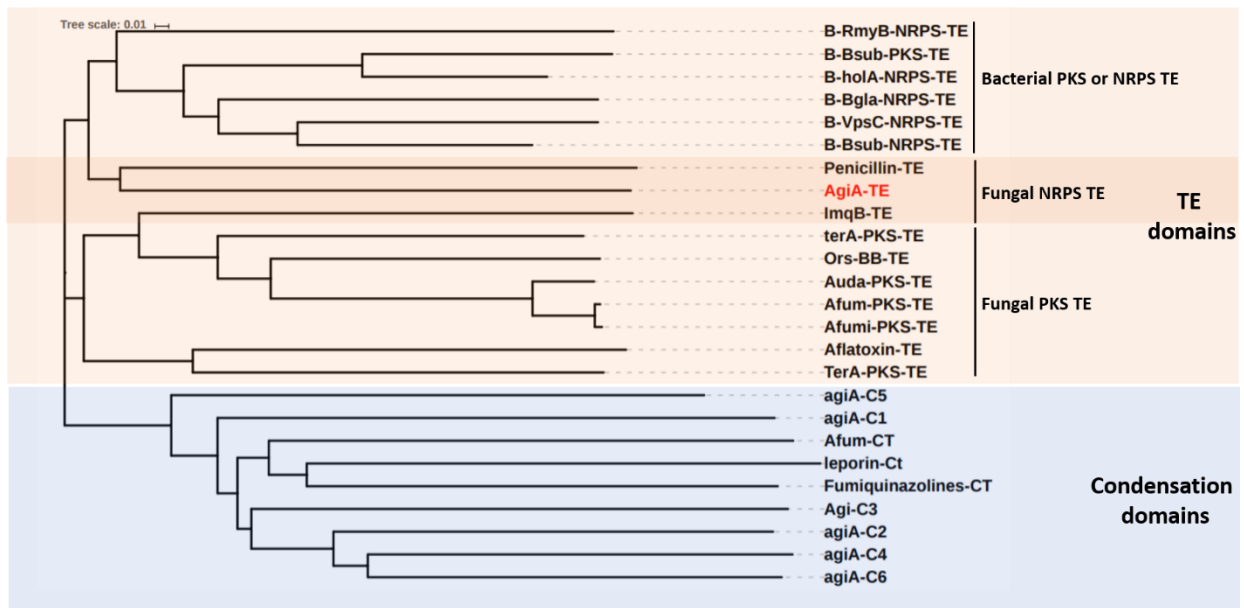
```

191

192 Figure S8. Multiple sequence alignment done using Clustal Omega. Red box highlights conserved motif.

193 Analysis of the thioesterase (TE) domains

194 Phylogenetic analysis of the *agiA* TE domain was done using Clustal Omega and iTOL with
195 defaults parameters (Figure S9). The TE domain is clearly distinct from condensation domains.
196 There is not a clear distinction among bacterial TE domains in PKS or NRPS genes. In contrast,
197 fungal TE domains in PKS genes are clustered together. Not many TE domains from fungal NRPS
198 are available, but *agiA*-TE is very closely related to another fungal NRPS-TE involved in the
199 biosynthesis of penicillin. Interestingly, the two fungal NRPS-TE clustered more closely to the
200 bacterial TE domains than the fungal PKS TE domains.



201
202 **Figure S9.** Phylogenetic tree for the TE domains (orange) and C domains (blue). Dark orange highlights fungal NRPS-
203 TE domains. The TE domains is divided in bacterial TEs, fungal NRPS-TE and fungal PKS-TE domains.

204 Fungal transformation

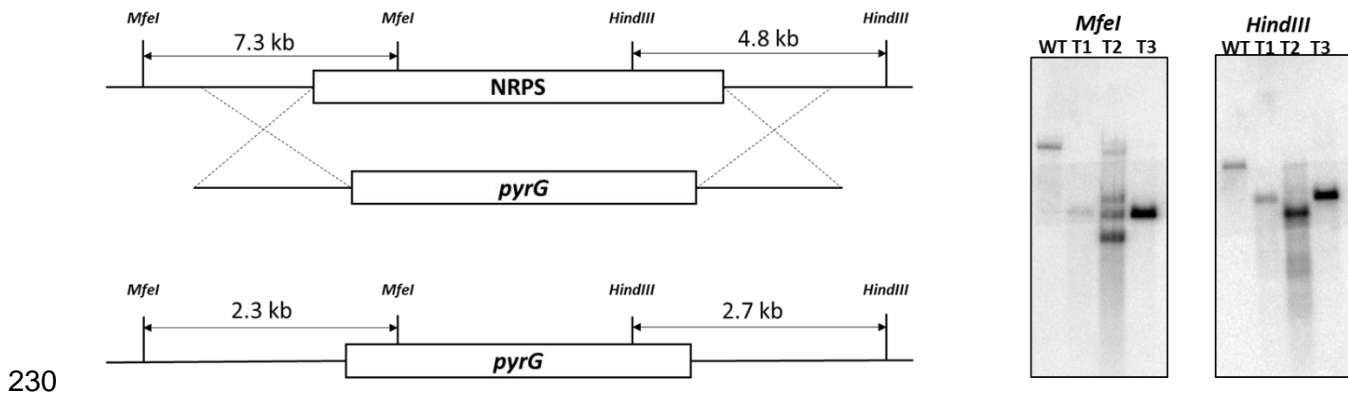
205 A fresh spore suspension (2×10^6 spores/mL) of TXZ13 was used to inoculate 500 mL of sterile
206 GMM and shaken at 280 rpm and 28 °C until the formation of young germlings (~13 hours). The
207 germlings were centrifuged at 8000 rpm for 15 mins at 4 °C. The supernatant was discarded and
208 50 mL of sterile dH₂O water was added to the germlings. They were spin at 8000 rpm for 15 mins
209 at 4 °C. The supernatant was removed and the germlings were transferred to 10 mL of osmotic
210 medium (1.2 M MgSO₄, 10 mM NAPB*), adjusted to pH 5.8 with 1 M Na₂HPO₄) with 30 mg of
211 Lysing Enzymes (Sigma) and 20 mg of Yatalase (TaKaRa). The germlings were then shaken at
212 80 rpm and 28 °C, until protoplasts were obtained (approx. 3 h). The protoplast solution (10 mL)
213 were transferred to a 30 mL cortex tube and very gently overlaid with 10 mL of trapping buffer

214 (0.6 M sorbitol and 0.1 M Tris-HCl, pH 7.0). After centrifugation in the HB-4 (or Beckmann
215 equivalent) rotor at 5000 rpm for 15 min at 4 °C, the protoplasts were removed from the interface
216 and transferred to a 15 mL sterile tube. The protoplasts were diluted with one volume of STC
217 buffer (1.2 M sorbitol, 10 mM CaCl₂, 10 mM Tris-HCl, pH 7.5) and centrifuged at 6000 rpm for 10
218 min at 4 °C. The supernatant was removed, and the protoplasts were resuspended in STC (1-2
219 mL) and stored on ice. The transforming DNA (e.g. specific gene disruption construct) was diluted
220 with STC (10 µg/100 µL) in a 15 mL falcon tube. The protoplast was added to the DNA (100 µL)
221 and incubated on ice for 50 minutes. Then 1.25 mL of PEG solution (60% PEG 4000, 50 mM
222 CaCl₂, 50 mM 10 mM Tris-HCl, pH 7.5) was added, mixed gently and incubated at room
223 temperature for 20 minutes. Next 5 mL of STC was added to the mixture, gently mixed and the
224 entirety plated (500 µL) on GMM media containing sorbitol (1.2 M). Resulting transformants were
225 subcultured twice on selective media and confirmed by Southern and PCR.

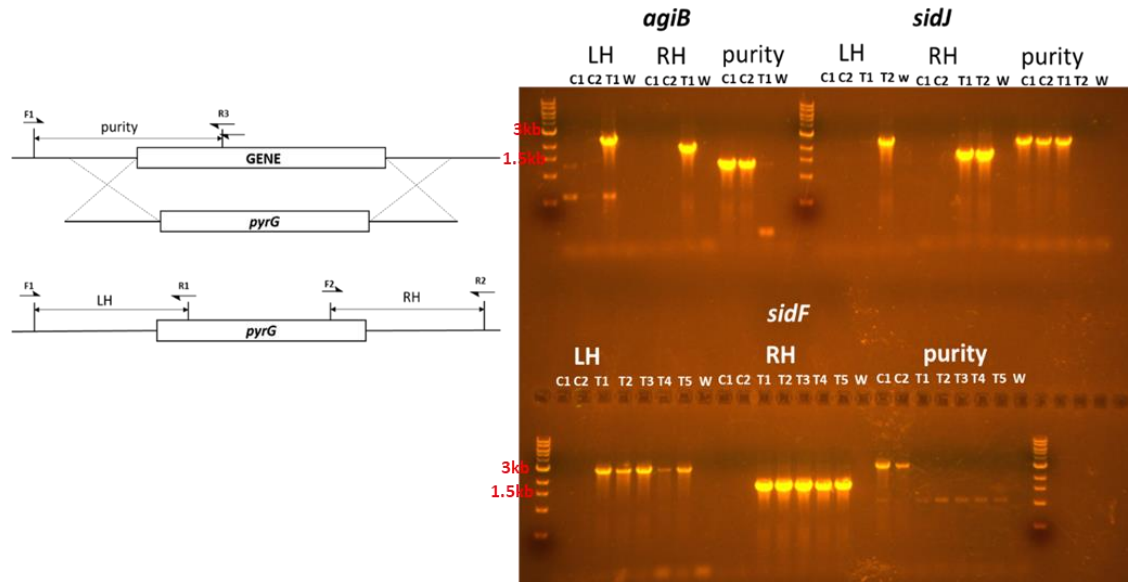
226 *NaPB: 2M phosphate buffer = 90.9 g Na₂HPO₄ and 163.4 g NaH₂PO₄ per liter, with pH 6.5.

227 Transformant confirmation

228 The transformants were confirmed using Southern analysis for the Δ *agiA* strain (Figure S10) and
229 PCR analysis for Δ *agiB*, Δ *sidJ* and Δ *agiF* (Figure S11). Primers used are listed on Table S3.



231 **Figure S10.** Schematic of the expected product from digestion using *MfeI* and *HindIII* (left). Southern results for Δ *agiA*.



232

233 **Figure S11.** PCR confirmation of the correct disruption of the resistance and purity. Schematic of the expected product
 234 (left). Gel for the transformants C = control; W = water, T = transformants. Purity test indicates primer that amplify the
 235 ORF, and no product should be observed in the correct transformants. $\Delta agiB$; T1 correct LH (2500 bp), RH (1744 bp),
 236 and no product in purity test (1286 bp). $\Delta sidJ$; T2 correct LH (2426 bp), RH (2005 bp), and no product in purity test
 237 (2490 bp). $\Delta agiB$; T1, T2, T3, T4, T5 correct LH (2861 bp), RH (1730 bp), and no product in purity test (3034 bp).

238 Reverse transcriptase quantitative PCR (RT-qPCR)

239 The wild- type and $\Delta sntB$ strains were grown in liquid PDB media at 30 °C and 200 rpm. RNA was
 240 extracted at day 2, 3 and 6 from lyophilized tissues using Trizol (Invitrogen). For RT-qPCR, RNA
 241 was quantified and 10 μ g was DNaseI treated before cDNA synthesis using iScript (Bio-Rad).
 242 Primers used in qPCR are listed (Table S2). qPCR was performed using iQ SYBR Green
 243 Supermix (BIO-RAD) and CFX Connect Real-Time System machine (BIO-RAD). Program used
 244 consisted of: (1) 95 °C for 3 minutes; (2) 95 °C for 30 seconds; (3) 55 °C for 30 seconds; Steps
 245 2-3 were repeated 39 times.

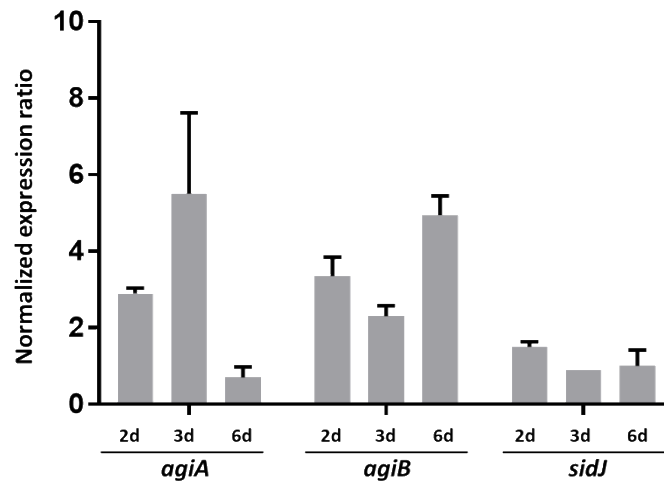
246 The relative quantification of gene expression using $2^{-\Delta\Delta C_T}$ (Livak) method. **(1)** The C_T value of the
 247 target gene from the $\Delta sntB$ was normalized to reference gene (actin). **(2)** Then the C_T from WT of
 248 the target gene was normalized to reference gene (actin). **(3-4)** The Normalized expression ratio
 249 was calculated.

250
$$(1) \Delta C_{T(test)} = C_{T(target, test)} - C_{T(ref., test)}$$

251
$$(2) \Delta C_{T(calibration)} = C_{T(target, calibrator)} - C_{T(ref., calibrator)}$$

252
$$(3) \Delta\Delta C_T = \Delta C_{T(test)} - \Delta C_{T(calibrator)}$$

253
$$(4) 2^{-\Delta\Delta C_T} = \text{Normalized expression ratio}$$

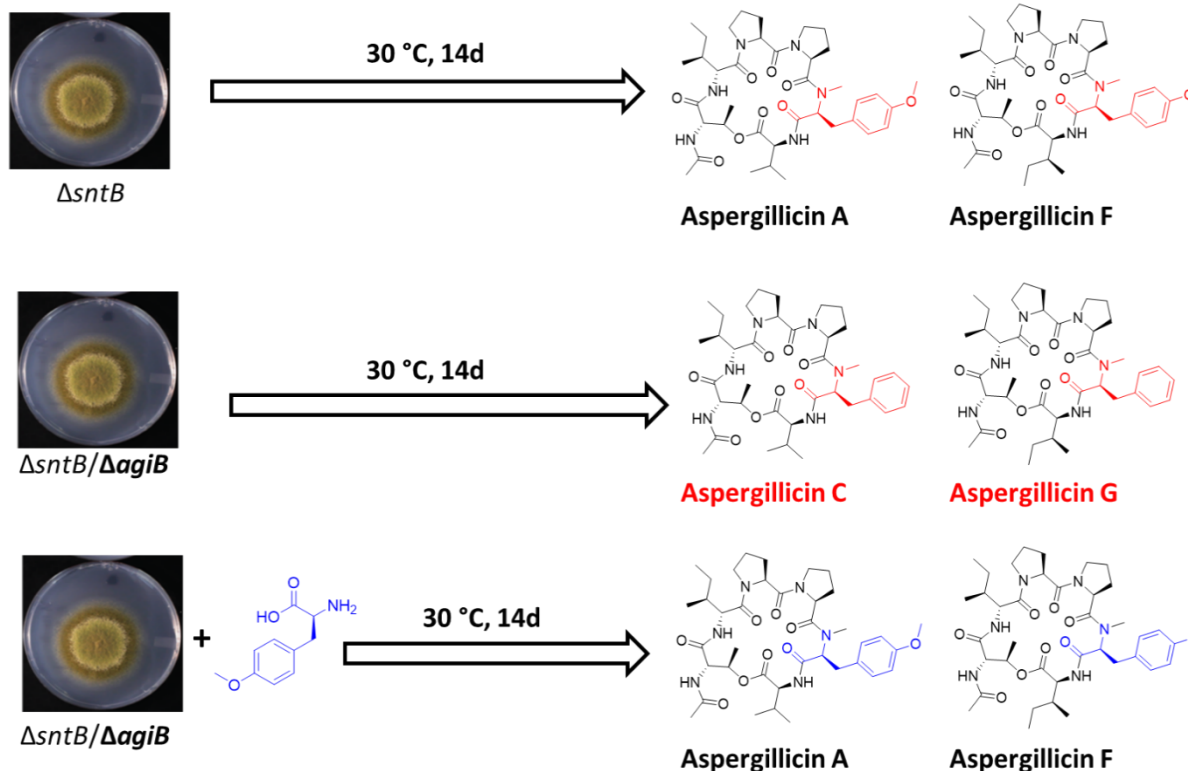


254

255 **Figure S12.** Bar charts showing relative expression of *agiA*, *agiB* and *sidJ* using normalized expression ratio ($2^{-\Delta\Delta Ct}$
 256 Method) between WT and $\Delta sntB$.

257 **Feeding experiment**

258 The $\Delta sntB/\Delta agiB$ strain was inoculated to six 500 mL flasks, each containing 200 mL of PDB.
 259 They were grown at 30 °C with shaking at 200 rpm. A solution of O-Me-L-tyrosine in water (200
 260 mg/10 mL) was divided over three flasks and added over three days (day 6, 7, 8). Each flask was
 261 extracted separately with ethyl acetated. The six extracts (three fed with O-Me-L-tyrosine) were
 262 analyzed by UPLC-HRMS (Figure S13).

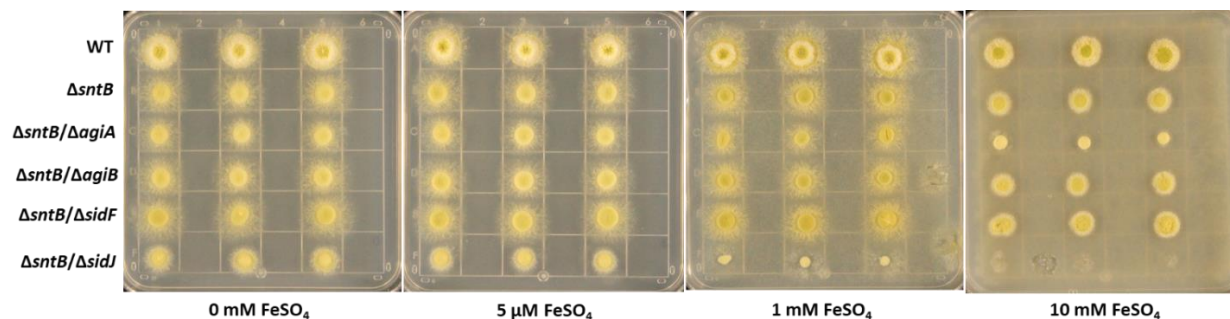


263

264 **Figure S13.** Summary of the feeding experiment using *O*-Me-L-tyrosine. *ΔsntB* produces aspergillicin A **1** and F **2**.
 265 *ΔsntBΔagiB* produces aspergillicin C **4** and aspergillicin G **11**. *ΔsntBΔagiB* plus *O*-Me-tyrosine produces aspergillicin A
 266 **1** and aspergillicin F **2**.

267 Sensitivity to iron experiment

268 The wild type and all the deletion strains were serially passaged for three times on GMM lacking
 269 iron and then plated on plates containing either no iron, normal growth media level of FeSO₄ (5
 270 μM), high level of FeSO₄ (1 mM) and very high level of FeSO₄ (10 mM). The plates were grown
 271 for 5 days at 30 °C and their growth was evaluated.

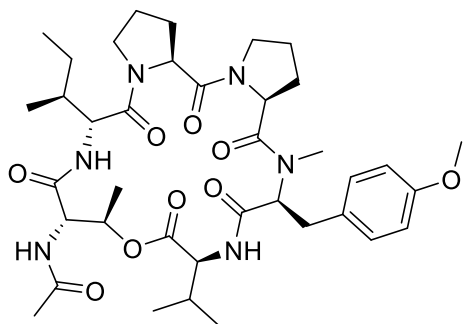


272

273 **Figure S14.** GMM plates containing different amounts of FeSO₄ (0, 5 μM, 1 mM and 10 mM) inoculated with WT and
 274 *ΔsntB*, *ΔsntBΔagiA*, *ΔsntBΔagiB*, *ΔsntBΔsidF* and *ΔsntBΔsidJ*. Picture taken after 5 days.

275 **Isolations of aspergillicins**

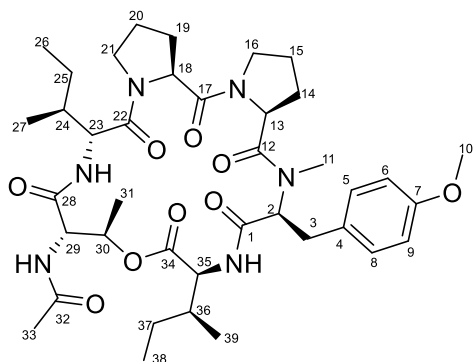
276 **Aspergillicin A 1**



277

278 *A. flavus* Δ *sntB* was grown on PDA plates (10 x 25 mL) at 30 °C. After 14 days, it was extracted
279 and purified using prep-HPLC to obtain of pure aspergillicin A 1 as faint yellow powder (1.6 mg).
280 λ_{\max} / nm 200, 220, 280; δ_{H} (CDCl₃, 600 MHz) 8.25 (1H, d, 8.5 Hz), 7.10-7.08 (1H, m), 7.04 (2H,
281 d, 8.5 Hz), 6.84 (2H, d, 8.5), 6.62 (1H, d, 9.5 Hz), 5.56 (1H, m), 4.95 (1H, dd, 11.5, 3.3 Hz), 4.86
282 (1H, dd, 10.0, 2.5 Hz), 4.62 (1H, dd, 9.5, 7.2 Hz), 4.52 (1H, dd, 9.2, 5.2 Hz), 4.42 (1H, dd, 8.5, 5.9
283 Hz), 4.32 (1H, dd, 8.5, 5.2), 3.78(3H, s), 3.70-3.63 (2H, m), 3.58-3.49 (2H, m), 2.16 (3H, s), 2.20-
284 2.08 (3H, m), 2.0-1.8 (4H, m), 1.74-1.70 (2H, m), 1.39-1.37 (1H, m), **1.30** (3H, m), **1.0-0.85** (13H,
285 m); δ_{C} (CDCl₃, 150 MHz) 173.4, 171.3, 171.25, 170.4, 170.2, 169., 168.6, 130.7 (2C), 130.5, 114.5
286 (2C), **72.0**, 62.7, 59.0, 58.4, 47.6, 47.5, **47.8**, 38.1, 33.6, 30.5, 29.5, **28.7**, **28.0**, **26.2**, **25.6**, **24.8**,
287 **23.**, **19.6**, **18.4**, **16.7**, **14.3**, **11.9**; m/z (ESI) 741.4175 [M+H]⁺ (C₃₈H₅₆N₆O₉ requires 741.4187).
288 Data in accordance to the literature.⁸ chemical shifts in **bold** were identified using HSQC/HMBC.

289 **Aspergillicin F 2**

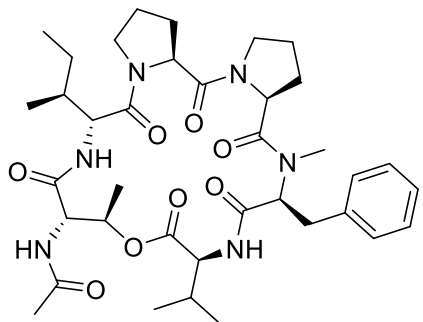


290

291 *A. flavus* Δ *sntB* was grown on PDA plates (10 x 25 mL) at 30 °C. After 14 days, it was extracted
292 and purified using prep-HPLC to obtain of pure aspergillicin F 2 as faint yellow powder (8 mg).

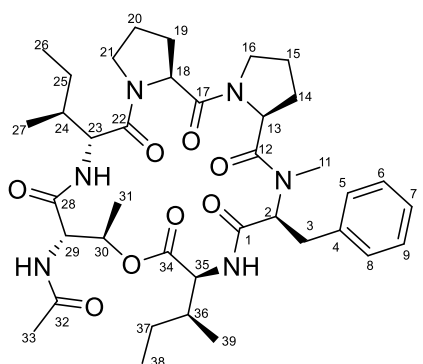
293 λ_{\max} / nm 200, 220, 280; δ_{H} (CDCl₃, 600 MHz) and δ_{C} (CDCl₃, 150 MHz) see Table S4; m/z (ESI)
294 755.4337 [M+H]⁺ (C₃₉H₅₈N₆O₉ requires 755.4343). Data in accordance to the literature.⁸

295 **Aspergillicin C 4**



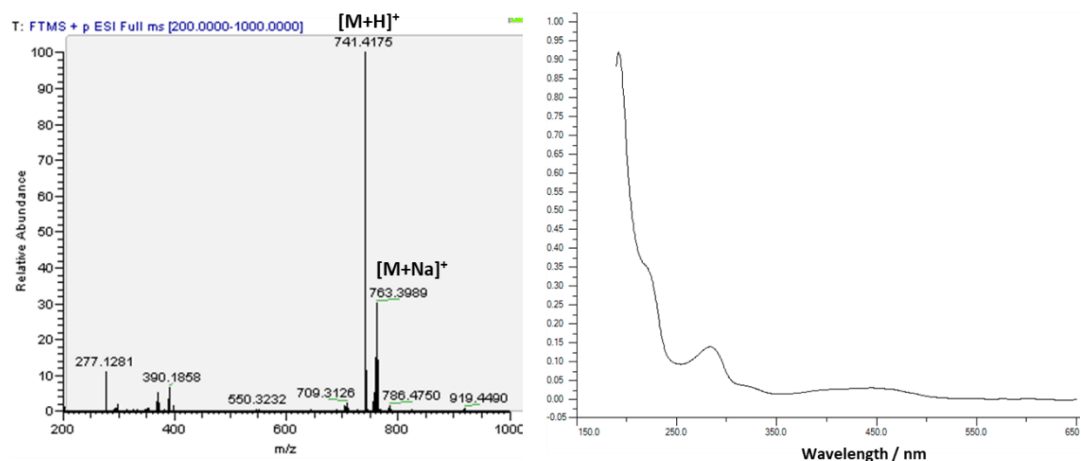
296
297 *A. flavus* $\Delta\text{sntB}\Delta\text{agiB}$ was grown on PDA plates (10 x 25 mL) at 30 °C. After 14 days, it was
298 extracted and purified using prep-HPLC to obtain of pure aspergillicin C 4 as faint yellow powder
299 (1 mg). λ_{\max} / nm 200, 220, 280; δ_{H} (CDCl₃, 600 MHz) 8.26 (1H, d, 8.0 Hz), 7.33-7.26 (3H, m),
300 7.21-7.10 (3H, m), 6.63 (1H, d, 9.7 Hz), 5.60-5.54 (1H, m), 5.01 (1H, dd, 11.8, 3.6), 4.87,(1H, dd,
301 10.0, 2.4 Hz), 4.63 (1H, dd, 9.6, 7.5 Hz), 4.51 (1H, m), 4.41 (1H, dd, 8.6, 6.2 Hz), 4.27 (1H, m),
302 3.70-3.47 (4H, m), 3.22, (1H, dd, 14.2, 3.0 Hz), 3.04 (1H, dd, 14.2, 11.5), 2.85 (3H, s), 2.17 (3H,
303 s), 2.25-2.18 (2H, m), 2.01-1.84 (4H, m), 1.70-1.62 (2H, m), 1.43-1.38 (1H, m), 1.27 (3H, d, 15
304 Hz), 1.16-1.09 (1H, m), 1.8-0.75 (14H, m); m/z (ESI) 711.4072 [M+H]⁺ (C₃₇H₅₄N₆O₈ requires
305 711.4081). Data in accordance to the literature.⁹

306 **Aspergillicin G 11**



307
308 *A. flavus* $\Delta\text{sntB}\Delta\text{agiB}$ was grown on PDA plates (10 x 25 mL) at 30 °C. After 14 days, it was
309 extracted and purified using prep-HPLC to obtain of pure aspergillicin G 11 as faint yellow powder
310 (5 mg). λ_{\max} / nm 200, 220, 280; ¹H NMR and ¹³C NMR data see Table S5; m/z (ESI) 725.4232
311 [M+H]⁺ (C₃₈H₅₆N₆O₈ requires 725.4237).

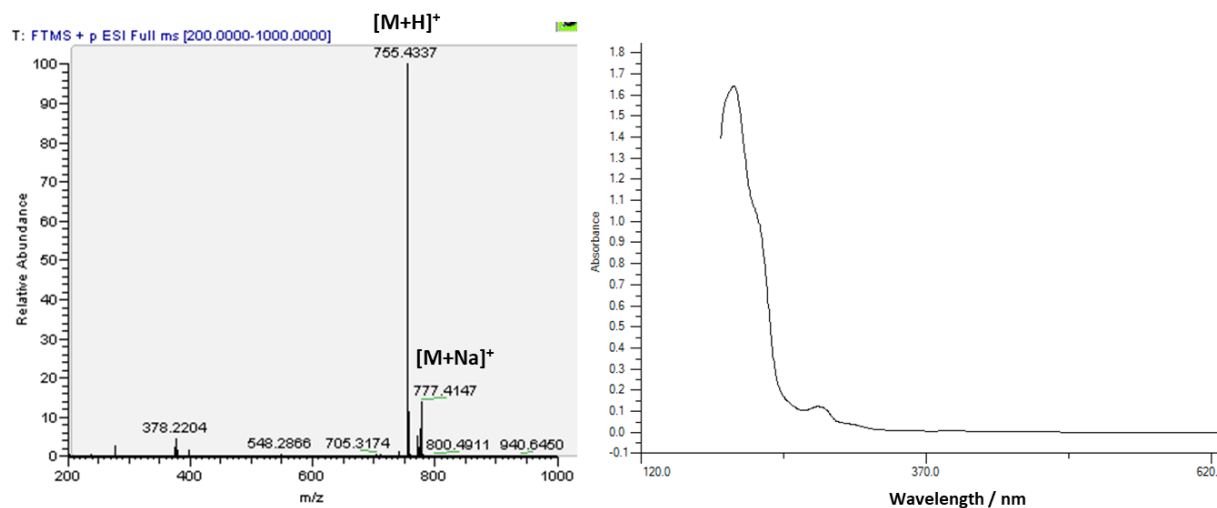
312 HRMS and UV spectra



313

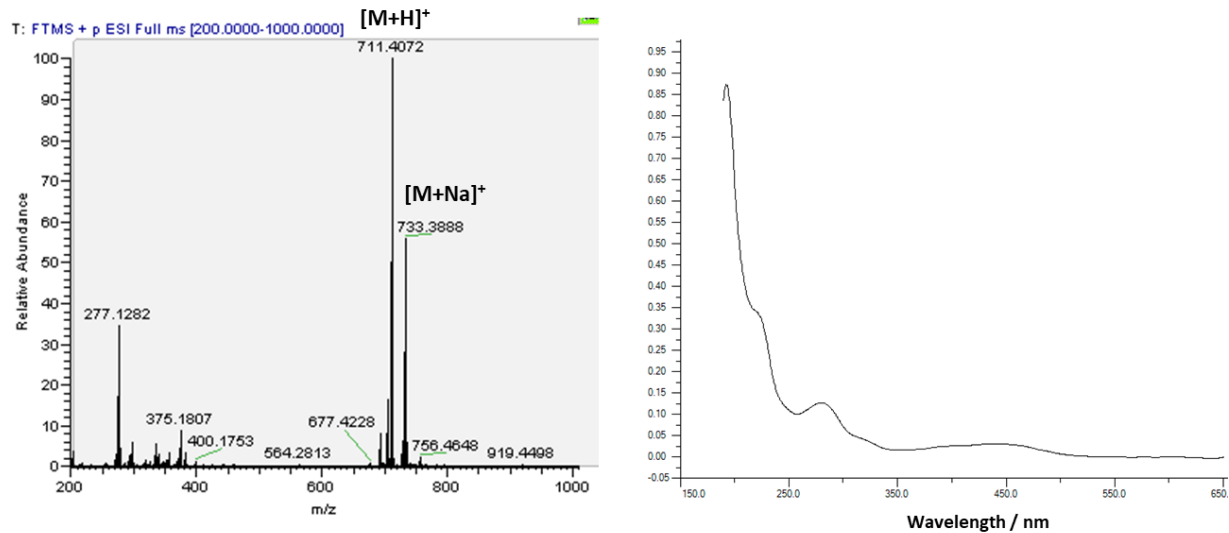
314 Figure S15. HRMS spectrum (left) and UV spectrum of aspergillicin A 1.

315 Aspergillicin F



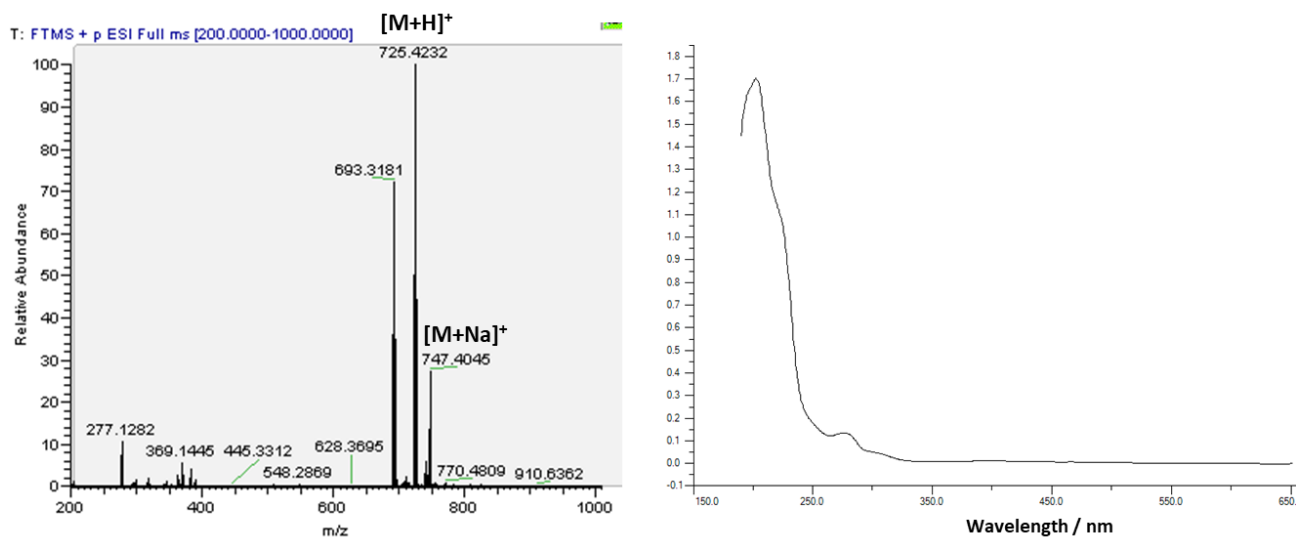
316

317 Figure S16. HRMS spectrum (left) and UV spectrum of aspergillicin F 2.



318

319 **Figure S17.** HRMS spectrum (left) and UV spectrum of aspergillicin B 4.



320

321 **Figure S18.** HRMS spectrum (left) and UV spectrum of aspergillicin G 11.

322

323

324

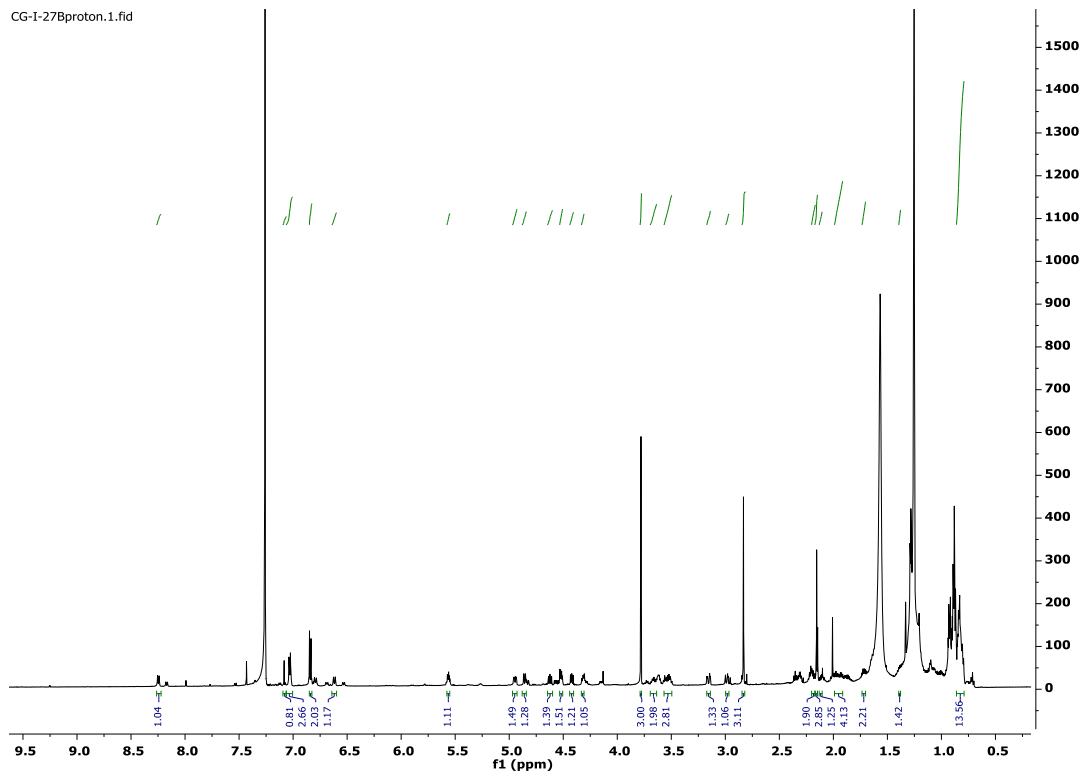
325

327 Table S4. NMR assignment of aspergillicin F 2 in agreement with literature⁸ (^a150 MHz, ^b600 MHz in CDCl₃).

Aspergillicin F			
Residue	Position	δ_c^a / ppm	δ_H^b / ppm (J in Hz)
<i>N</i> -Me-L- <i>O</i> -Me-Tyr	1	169.8	-
	2	62.7	4.95 (1H, dd, 11.5, 3.4)
	3a	33.7	3.17 (1H, dd, 14.7, 3.4)
	3b		2.98 (1H, dd, 14.7, 11.5)
	4	129.8	-
	5/9	130.6	7.03 (2H, d, 8.6)
	6/8	114.5	6.84 (2H, d, 8.6)
	7	158.9	-
	10	55.6	3.78 (3H, s)
	11	29.5	2.83 (3H, s)
L-Pro	12	173.4	-
	13	55.3	4.31 (1H, dd, 8.0, 5.0)
	14a	28.7	1.07 (1H, m)
	14b		0.87 (1H, m)
	15a	25.5	2.11 (1H, m)
	15b		1.71 (1H, m)
	16a	47.6	3.62 (1H, m)
	16b		3.52 (1H, m)
L-Pro	17	170.2	-
	18	58.3	4.51 (1H, dd, 8.5, 5.2)
	19a	28.1	2.20 (1H, m)
	19b		1.84 (1H, m)
	20a	24.8	1.98 (1H, m)
	20b		1.93 (1H, m)
	21a	47.8	3.7 (1H, m)
	21b		3.6 (1H, m)
<i>D</i> - <i>allo</i> -Ile	22	171.3	-
	23	54.9	4.61 (1H, dd, 9.9, 8.0)
	23-NH	-	6.54 (1H, d, 9.90)
	24	37.8	1.67 (1H, m)
	25	26.2	1.38 (1H, m)
			1.07 (1H, m)
	26	11.9	0.91 (3H, m)
	27	14.7	0.88 (3H, m)
<i>O</i> -Ac-L-Thr	28	168.8	-
	29	55.9	4.85 (1H, dd, 9.8, 2.2)
	29-NH	-	7.03 (1H, m)
	30	71.6	5.56 (1H, dq, 6.6, 2.2)
	31	16.8	1.28 (3H, d, 6.6)
	32	171.25	-
	33	23.3	2.14 (3H, s)
L-Ile	34	170.4	-
	35	57.7	4.55 (1H, dd, 8.8, 5.6)
	35-NH	-	8.17 (1H, d, 8.8)
	36	37.0	1.95 (1H, m)
	37	24.8	1.38 (1H, m)
			1.14 (1H, m)
	38	11.3	0.83 (3H, t, 7.4)
	39	15.8	0.90 (3H, m)

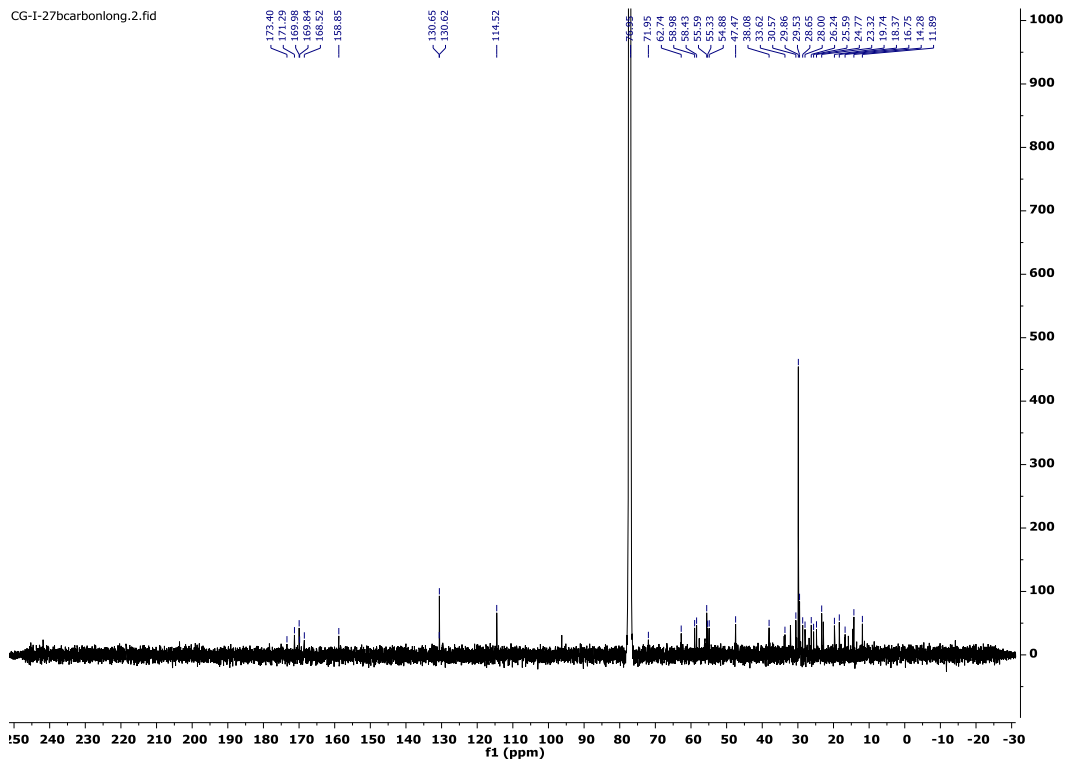
329 **Table S5.** NMR assignment of aspergillicin G **11** (^a150 MHz, ^b600 MHz in CDCl₃).

Aspergillicin G					
Residue	Position	δ_c^a / ppm	δ_H^b / ppm (J in Hz)	HMBC	COSY
N-Me-L-Phe	1	169.9	-	-	-
	2	62.7	5.00 (1H, dd, 11.5, 3.3)	C1	3a/3b
	3a	34.6	3.23 (1H, dd, 14.5, 3.3)	C1, C4, C5/9	2, 3b
	3b		3.03 (1H, dd, 14.5, 11.5)		2, 3a
	4	138.0	-	-	-
	5/9	129.1	7.13 (2H, m)	C3, C7	6/8, 7
	6/8	129.7	7.31 (2H, m)	C7, C5/9	5/9, 7
	7	127.2	7.25 (1H, m)	C5/9	6//8, 5/9
	11	29.9	2.85 (3H, s)	C12	-
L-Pro	12	173.4	-	-	-
	13	55.3	4.27 (1H, dd, 8.0, 5.0)	C14, C15	14a/b
	14a	28.6	0.97 (1H, m)	C12, C13,	13, 14b, 15a, 15b
	14b		0.71 (1H, m)		13, 14a, 15a, 15b
	15a	25.5	2.11 (1H, m)	C14, C13	15a, 15b, 16a, 16b
	15b		1.71 (1H, m)		15a, 15b, 16a, 16b
	16a	47.6	3.62 (1H, m)	C14, C13,	15a, 15b, 16b
	16b		3.52 (1H, m)		15a, 15b, 16a
L-Pro	17	170.2	-	-	-
	18	58.3	4.50 (1H, dd, 8.5, 5.2)	C17, C19, C20	19a/19b
	19a	28.0	2.20 (1H, m)	C17, C20, C21	18, 19b
	19b		1.84 (1H, m)		
	20a	24.8	1.98 (1H, m)	C19, C21	18, 19a
	20b		1.93 (1H, m)		
	21a	47.8	3.69 (1H, m)	C19, C20	20a, 20b, 21b
	21b		3.62(1H, m)		20a, 20b, 21a
D-allo-Ile	22	171.3	-	-	-
	23	55.0	4.62 (1H, dd, 9.9, 8.0)	C22, C24, C25, C27, C28	23NH, 24
	23-NH	-	6.56 (1H, d, 9.90)	C28	23
	24	37.8	1.67 (1H, m)	C23	23, 25, 27
	25	26.2	1.38 (1H, m)	C24, C26, 27	24, 26, 27
			1.07 (1H, m)		
	26	11.8	0.91 (3H, m)	C23, C24, C25	25
	27	14.7	0.88 (3H, m)	C23, C24, C25	25
O-Ac-L-Thr	28	168.7	-	-	-
	29	55.9	4.83 (1H, dd, 9.8, 2.2)	C28	29-NH, 30
	29-NH	-	6.8 (1H, d, 9.8)	-	29
	30	71.7	5.57 (1H, qd, 6.4, 2.2)	C34	29, 31
	31	16.9	1.28 (3H, d, 6.4)	C29, C30	29
	32	171.12	-	-	-
	33	23.3	2.14 (3H, s)	C32	-
L-Ile	34	170.2	-	-	-
	35	57.8	4.56 (1H, dd, 8.6, 5.6)	C34, C36, C39	35-NH, 36
	35-NH	-	8.18 (1H, d, 8.6)	C34	35
	36	37.1	1.95 (1H, m)	-	35, 37a, 37b, 39
	37	24.89	1.38 (1H, m)	-	36, 37a, 38
			1.14 (1H, m)		36, 37b, 38
	38	11.3	0.83 (3H, t, 7.4)	C36, C38, C39C37,	37a, 37b
	39	15.8	0.90 (3H, m)	-	38



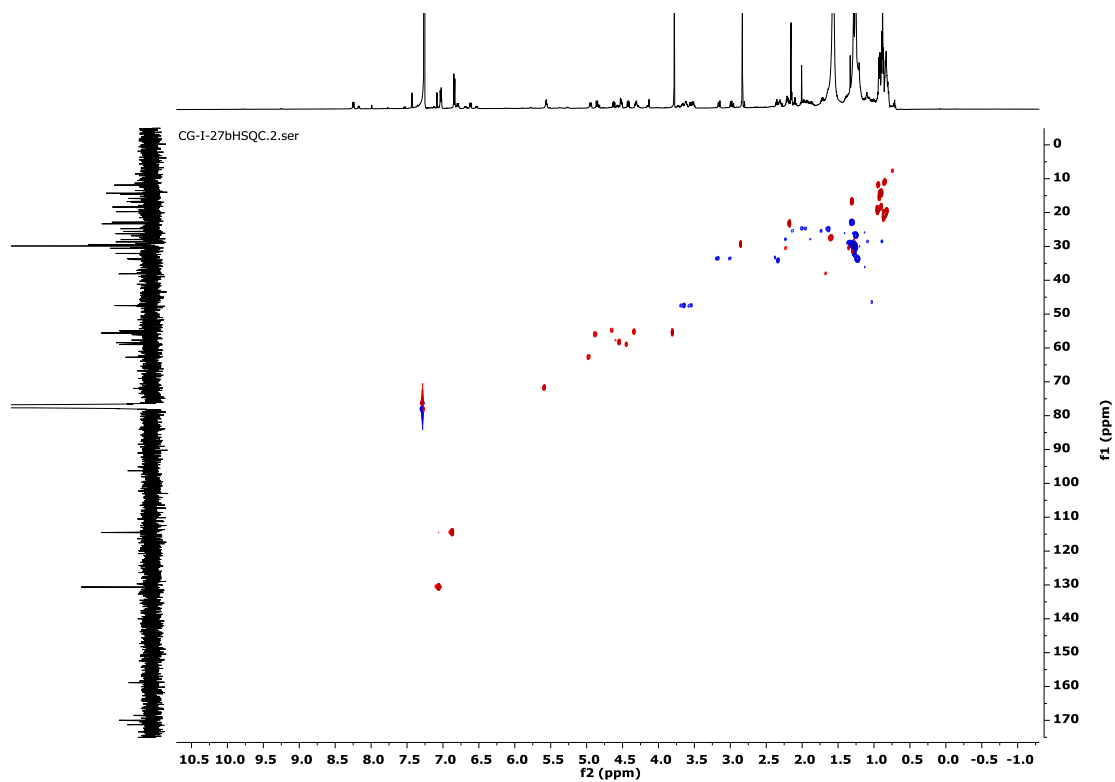
331

332 **Figure S19.** ^1H NMR of aspergillicin A 1 (600 MHz in CDCl_3).



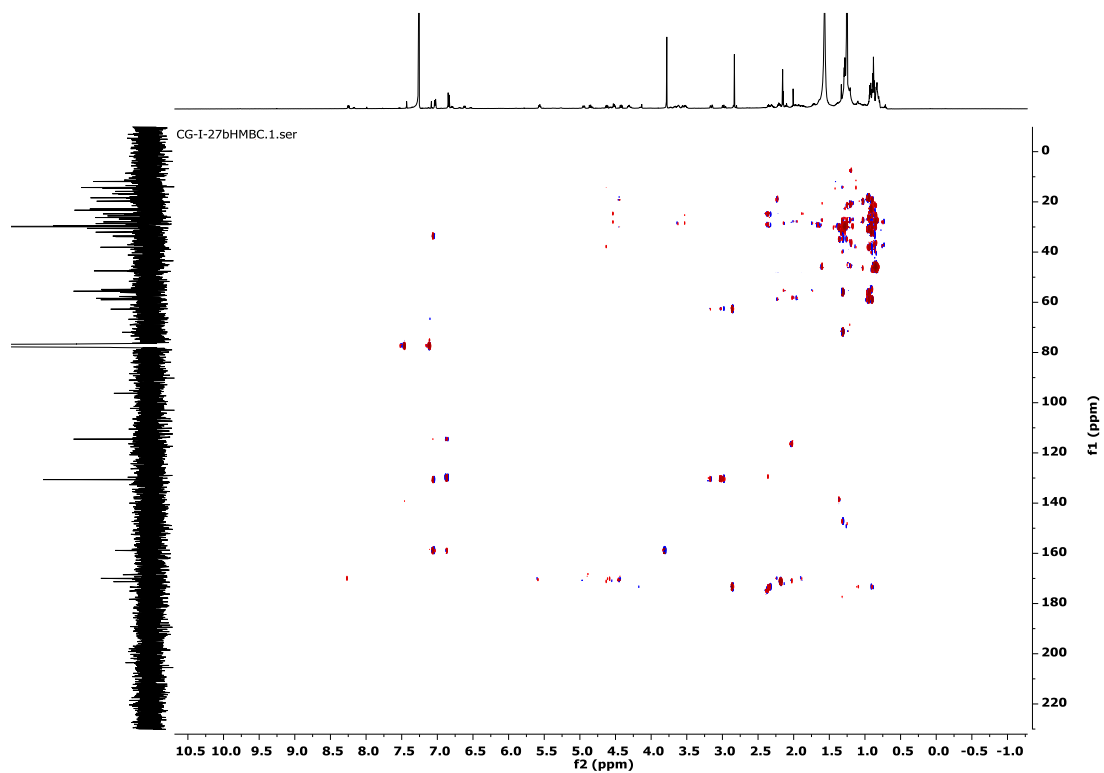
333

334 **Figure S20.** ^{13}C NMR of aspergillicin F 1 (150 MHz in CDCl_3)



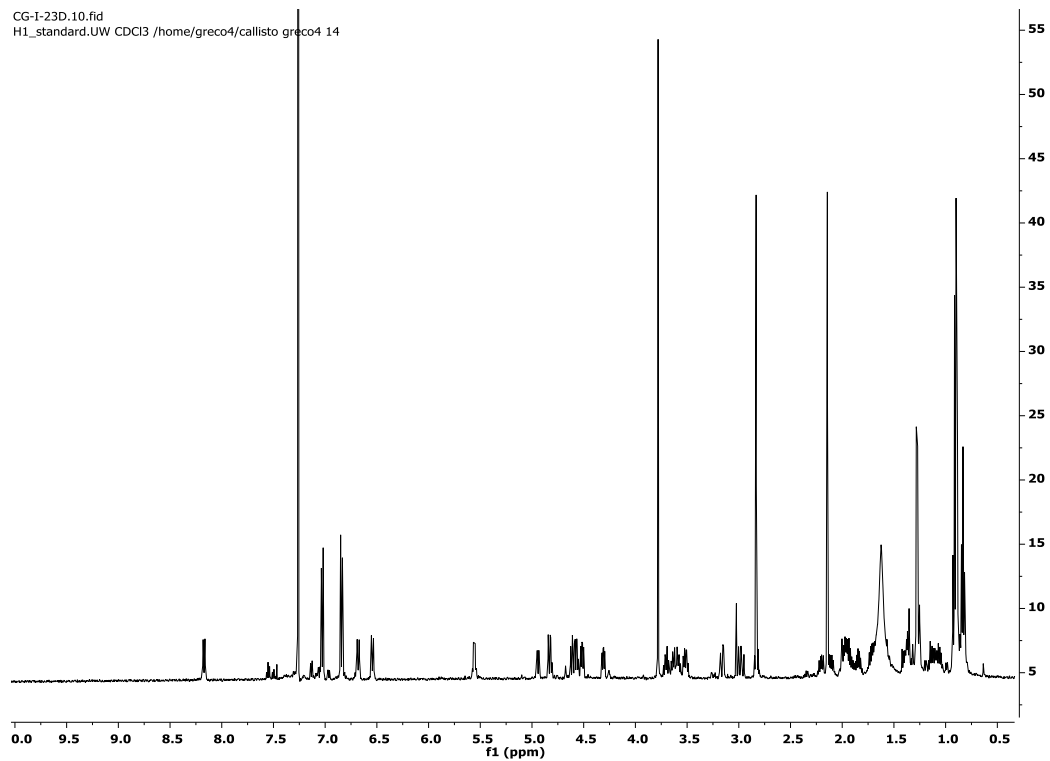
335

336 **Figure S21.** HSQC spectrum of aspergillicin A **1** (600 MHz in CDCl_3).



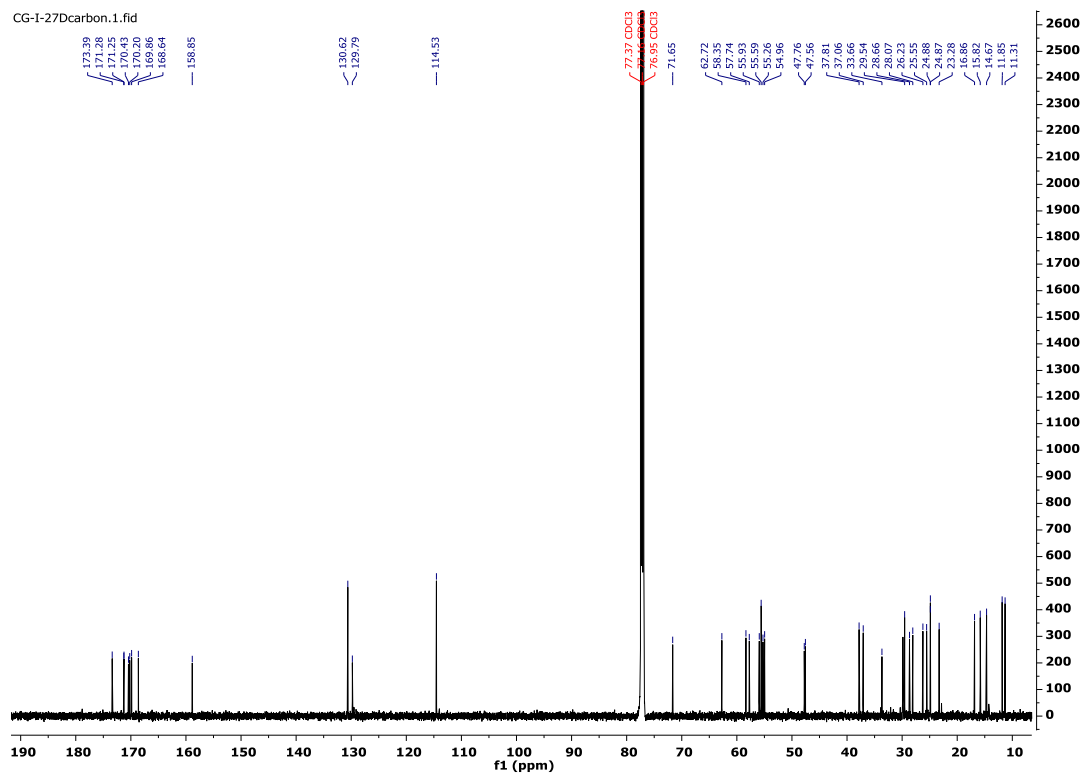
337

338 **Figure S22.** HMBC spectrum of aspergillicin A **1** (600 MHz in CDCl_3).



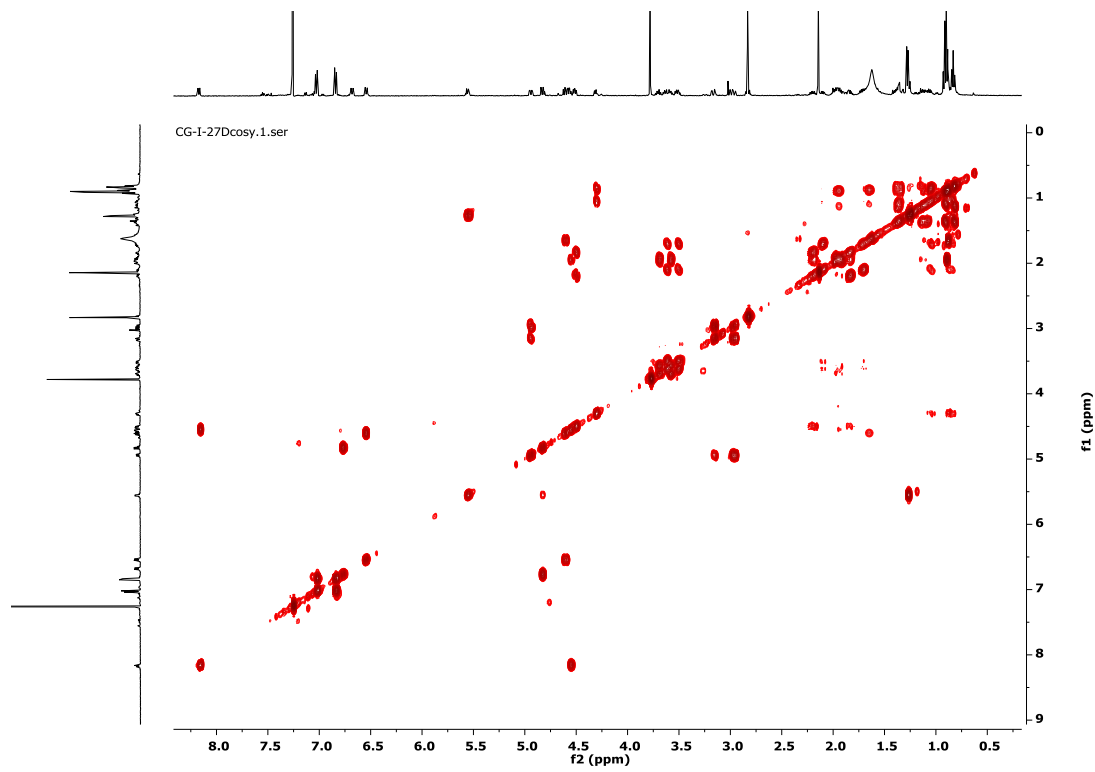
339

340 **Figure S23.** ^1H NMR of aspergillicin F 1 (600 MHz in CDCl_3).



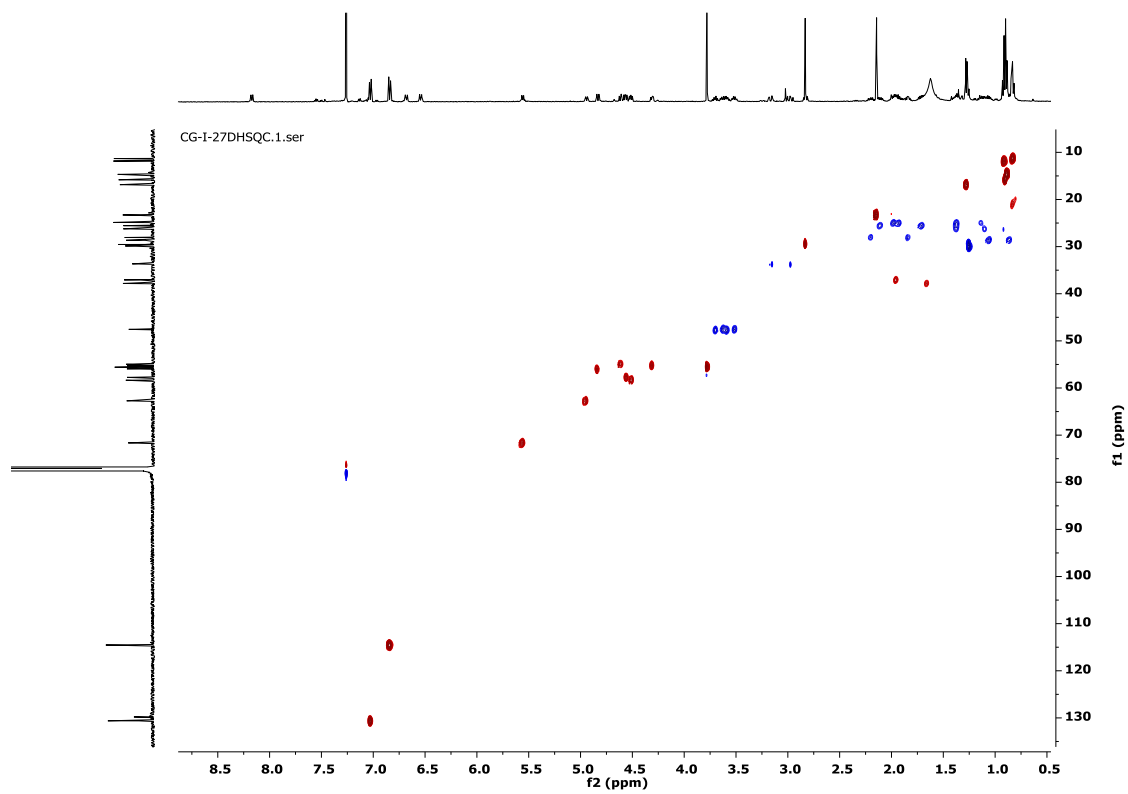
341

342 **Figure S24.** ^{13}C NMR of aspergillicin F 2 (150 MHz in CDCl_3)



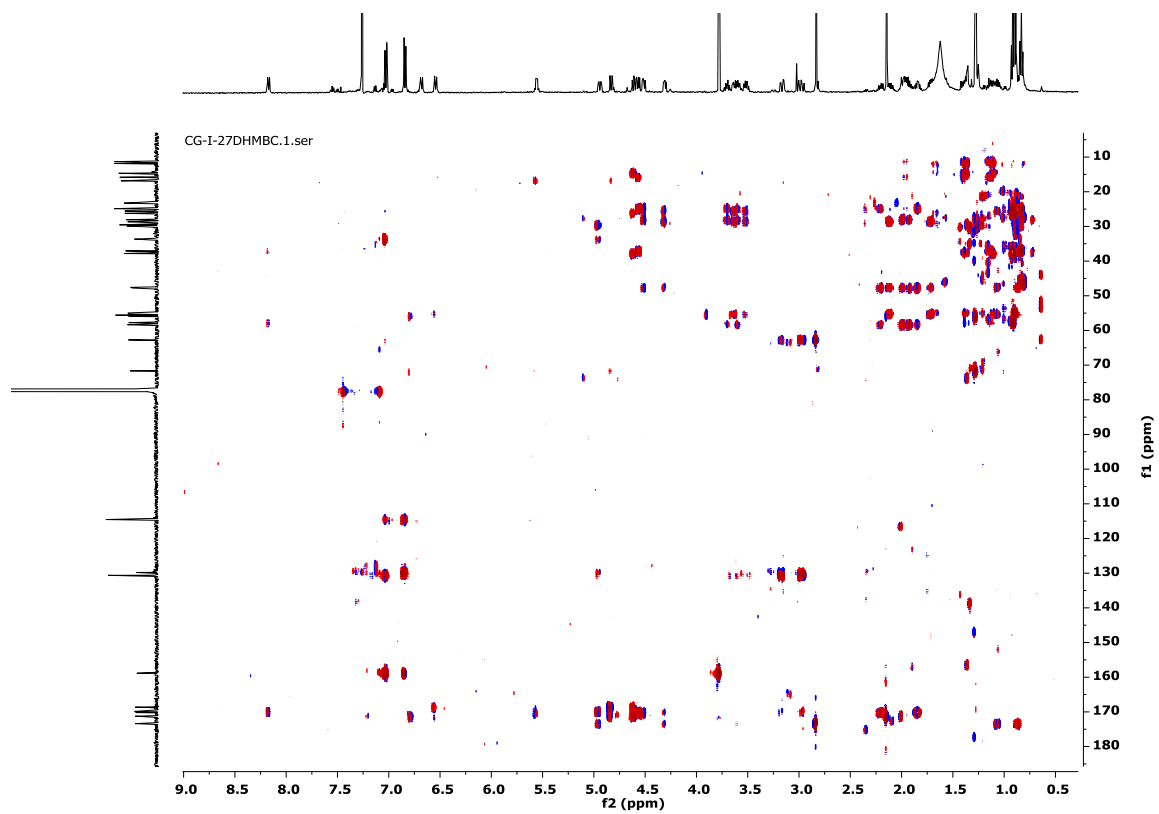
343

344 **Figure S25.** COSY spectrum of aspergillicin F 2 (600 MHz in CDCl₃).



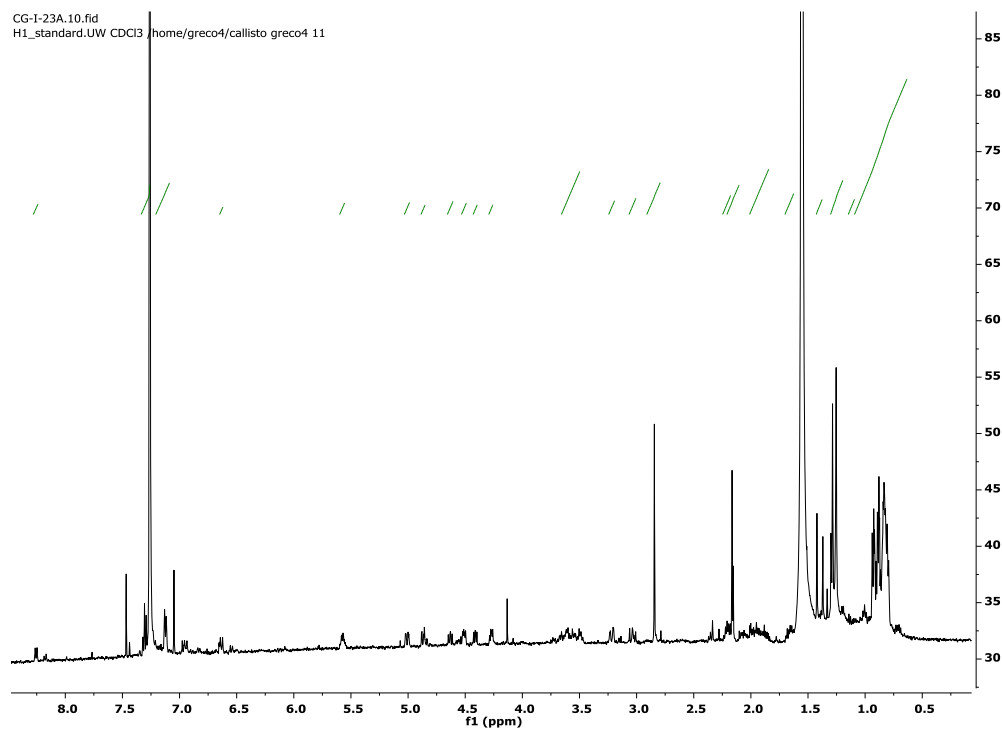
345

346 **Figure S26.** HSQC spectrum of aspergillicin F 2 (600 MHz in CDCl₃)



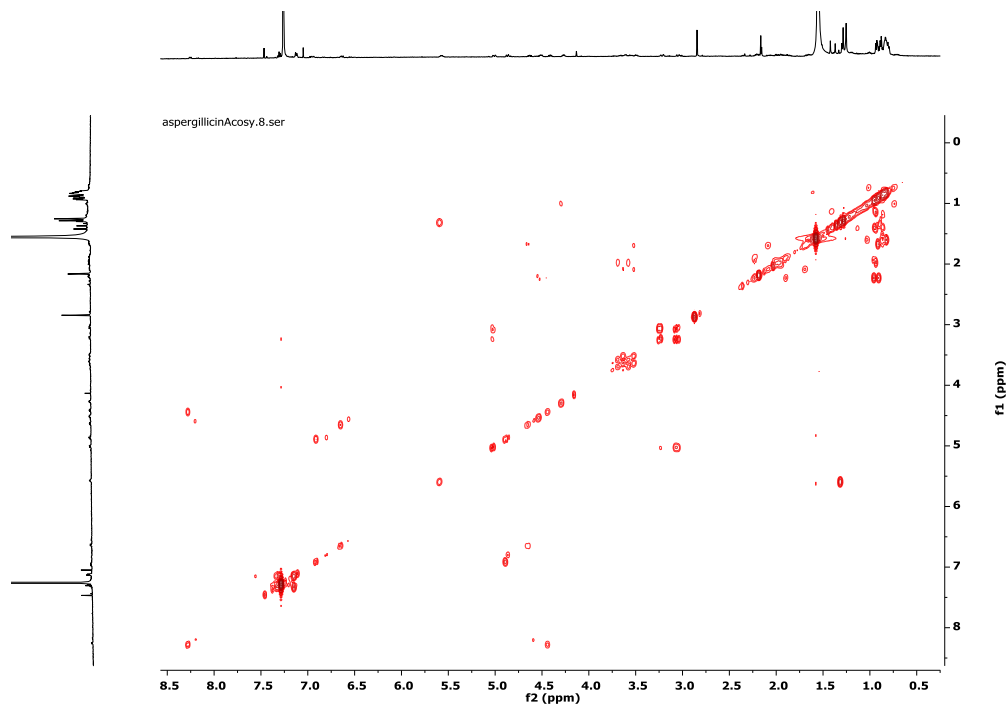
347

348 **Figure S27.** HMBC spectrum of aspergillicin F 2 (600 MHz in CDCl₃).



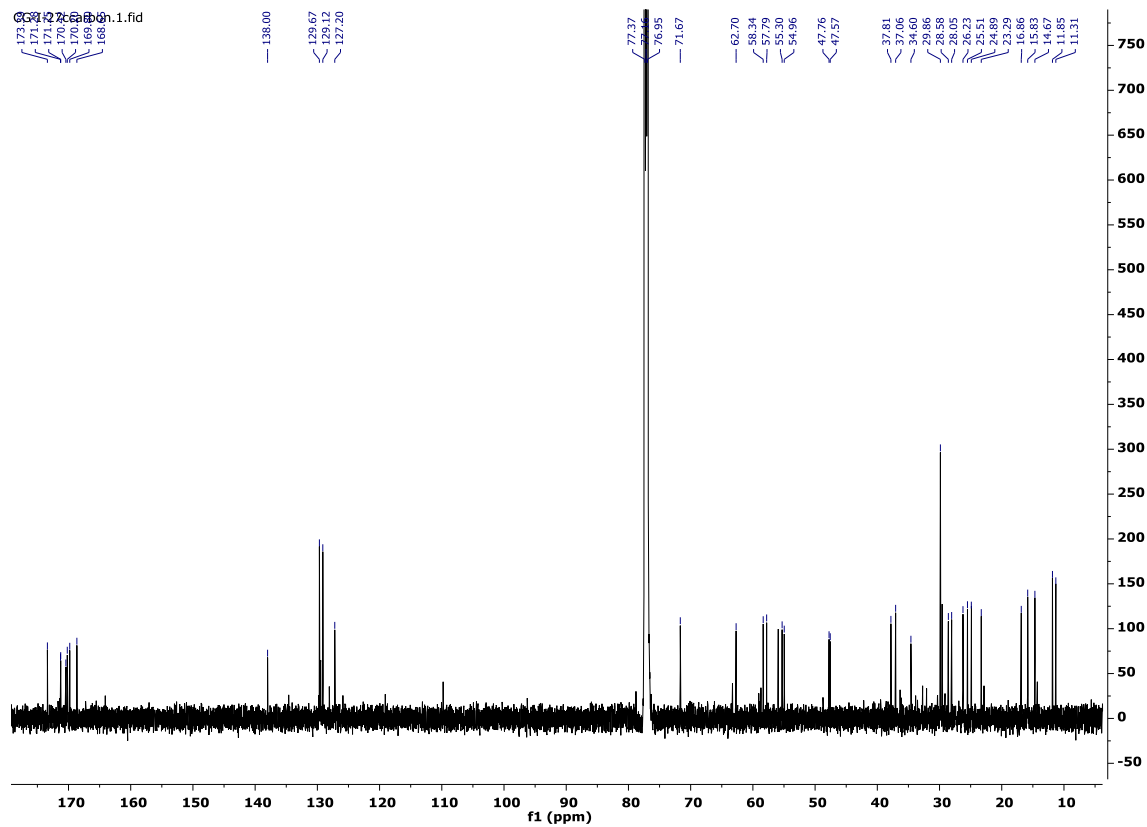
349

350 **Figure S28.** ¹H NMR of aspergillicin C 4 (600 MHz in CDCl₃).



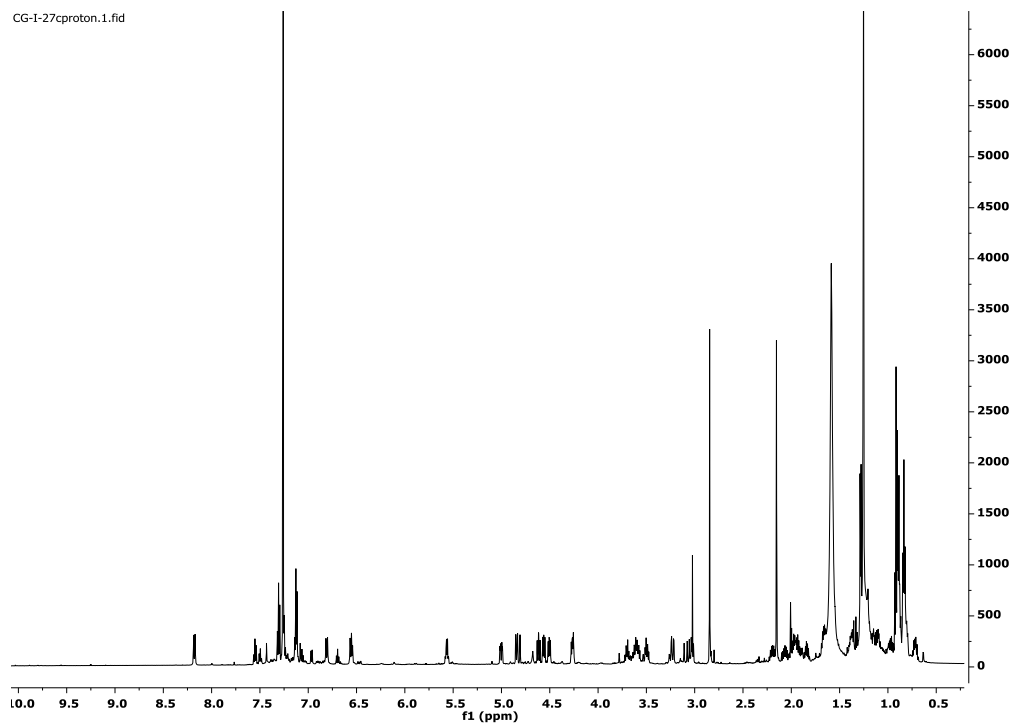
351

352 **Figure S29.** COSY spectrum of aspergillicin C 4 (600 MHz in CDCl_3).

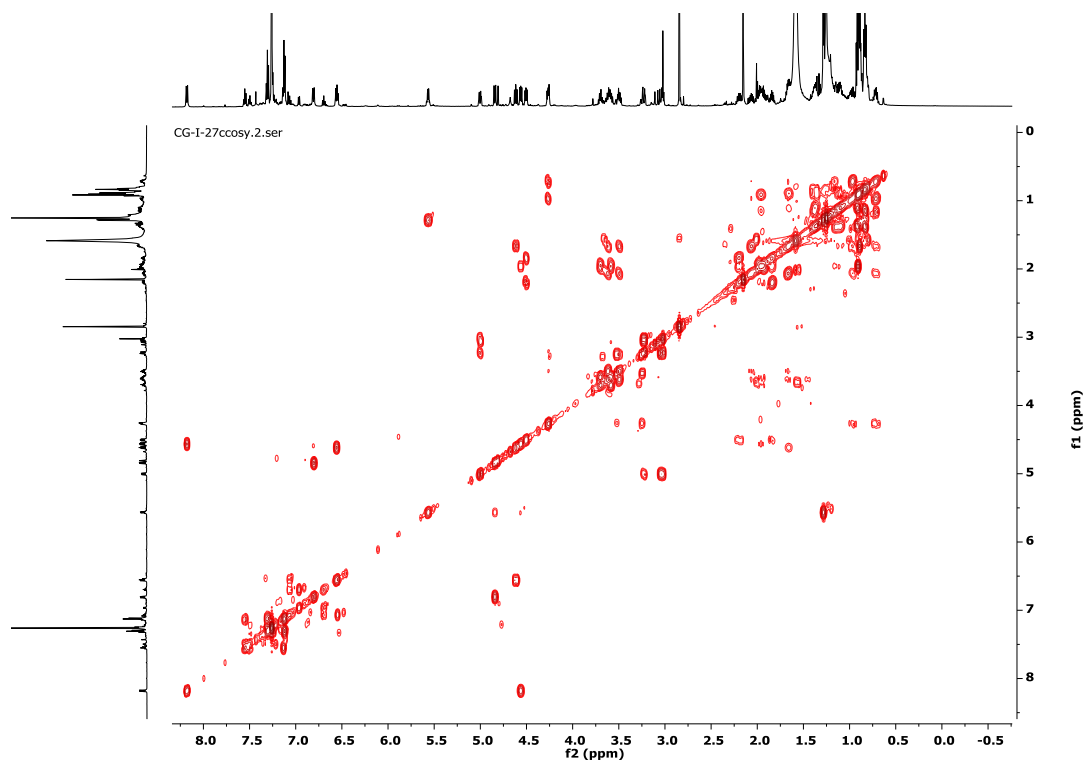


353

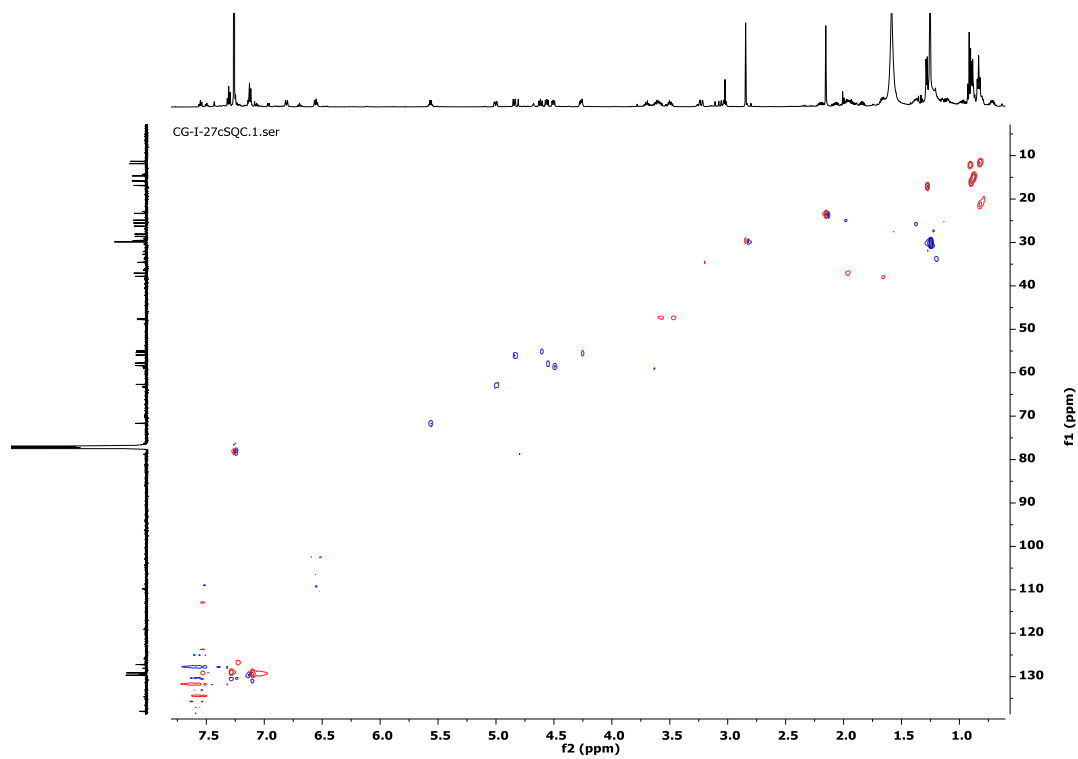
354 **Figure S30.** ^{13}C NMR of aspergillicin G 11 (150 MHz in CDCl_3).



356 **Figure S31.** ^1H NMR of aspergillicin G 11 (600 MHz in CDCl_3).

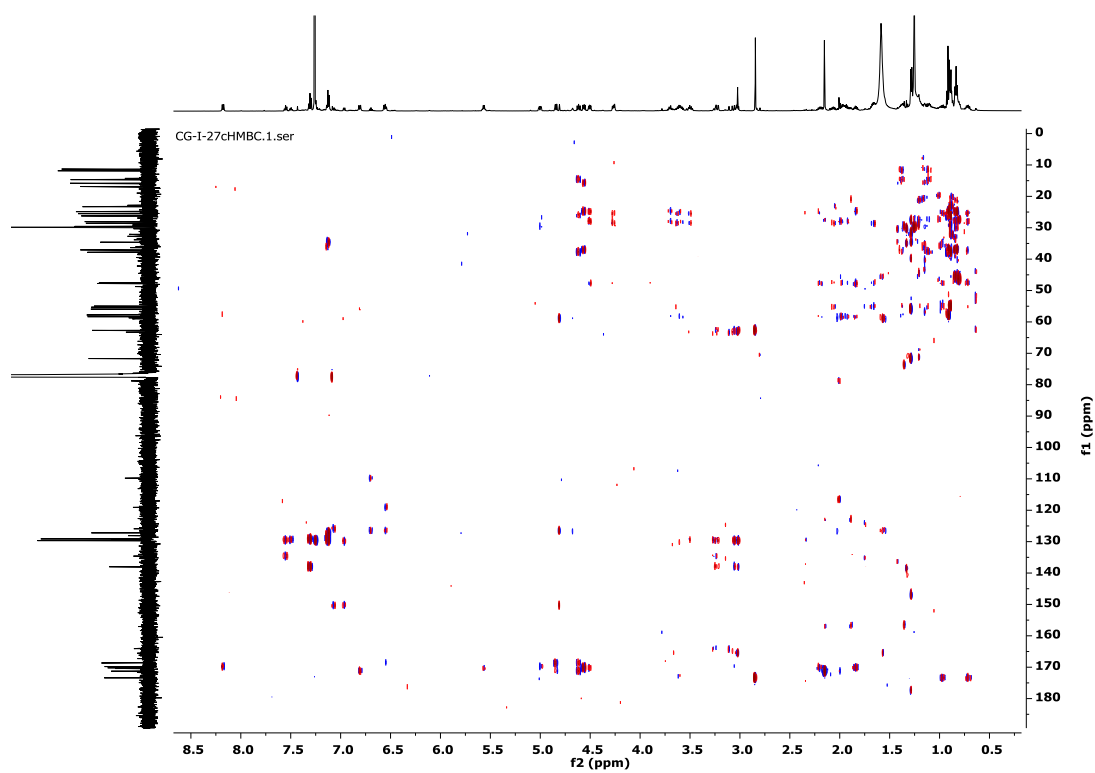


358 **Figure S32.** COSY spectrum of aspergillicin G 11 (600 MHz in CDCl_3).



359

360 **Figure S33.** HSQC spectrum of aspergillicin G **11** (600 MHz in CDCl₃).



361

362 **Figure S34.** HMBC spectrum of aspergillicin G **11** (600 MHz in CDCl₃).

363 **Reference**

- 364 (1) Shimizu, K.; Keller, N. P. Genetic Involvement of a CAMP-Dependent Protein Kinase in a
365 G Protein Signaling Pathway Regulating Morphological and Chemical Transitions in
366 *Aspergillus Nidulans*. *Genetics* **2001**, *157* (2), 591–600.
- 367 (2) Zhao, X.; Spraker, J. E.; Bok, J. W.; Velk, T.; He, Z.-M.; Keller, N. P. A Cellular Fusion
368 Cascade Regulated by LaeA Is Required for Sclerotial Development in *Aspergillus Flavus*.
369 *Front. Microbiol.* **2017**, *8*, 1925. <https://doi.org/10.3389/fmicb.2017.01925>.
- 370 (3) Pfannenstiel, B. T.; Zhao, X.; Wortman, J.; Wiemann, P.; Throckmorton, K.; Spraker, J. E.;
371 Soukup, A. A.; Luo, X.; Lindner, D. L.; Lim, F. Y.; et al. Revitalization of a Forward Genetic
372 Screen Identifies Three New Regulators of Fungal Secondary Metabolism in the Genus
373 *Aspergillus*. *MBio* **2017**, *8* (5), e01246-17. <https://doi.org/10.1128/mBio.01246-17>.
- 374 (4) Yu, J.-H.; Hamari, Z.; Han, K.-H.; Seo, J.-A.; Reyes-Domínguez, Y.; Scazzocchio, C.
375 Double-Joint PCR: A PCR-Based Molecular Tool for Gene Manipulations in Filamentous
376 Fungi. *Fungal Genet. Biol.* **2004**, *41* (11), 973–981.
377 <https://doi.org/10.1016/j.fgb.2004.08.001>.
- 378 (5) Carver, T. J.; Rutherford, K. M.; Berriman, M.; Rajandream, M.-A.; Barrell, B. G.; Parkhill,
379 J. ACT: The Artemis Comparison Tool. *Bioinformatics* **2005**, *21* (16), 3422–3423.
380 <https://doi.org/10.1093/bioinformatics/bti553>.
- 381 (6) Medema, M. H.; Takano, E.; Breitling, R. Detecting Sequence Homology at the Gene
382 Cluster Level with MultiGeneBlast. *Mol. Biol. Evol.* **2013**, *30* (5), 1218–1223.
383 <https://doi.org/10.1093/molbev/mst025>.
- 384 (7) Yelton, M. M.; Hamer, J. E.; Timberlake, W. E. Transformation of *Aspergillus nidulans* by
385 Using a TrpC Plasmid. *Proc. Natl. Acad. Sci. U. S. A.* **1984**, *81* (5), 1470–1474.
- 386 (8) Kikuchi, H.; Hoshikawa, T.; Fujimura, S.; Sakata, N.; Kurata, S.; Katou, Y.; Oshima, Y.
387 Isolation of a Cyclic Depsipeptide, Aspergillicin F, and Synthesis of Aspergillicins with Innate
388 Immune-Modulating Activity. *J. Nat. Prod.* **2015**, *78* (8), 1949–1956.
389 <https://doi.org/10.1021/acs.jnatprod.5b00286>.
- 390 (9) Capon, R. J.; Skene, C.; Stewart, M.; Ford, J.; O’Hair, R. A. J.; Williams, L.; Lacey, E.; Gill,
391 J. H.; Heiland, K.; Friedel, T. Aspergillicins A-E: Five Novel Depsipeptides from the Marine-
392 Derived Fungus *Aspergillus carneus*. *Org. Biomol. Chem.* **2003**, *1* (11), 1856–1862.

393 <https://doi.org/10.1039/b302306k>.

394

395